# ORIGINAL RESEARCH

Loss of H2R Signaling Disrupts Neutrophil Homeostasis and Promotes Inflammation-Associated Colonic Tumorigenesis in Mice

Zhongcheng Shi, PhD,[1,2,*] Yuko Mori-Akiyama, MD,[1,2,*] Wa Du, PhD,[3] Robert Fultz, PhD,[4] Yanling Zhao, PhD,[5] Wenly Ruan, MD,[6,7] Susan Venable,[1,2] Melinda A. Engevik, PhD,[1,2] and James Versalovic, MD, PhD[1,6,2]

[1]Department of Pathology and Immunology, Baylor College of Medicine, Houston, Texas; [2]Department of Pathology, Texas Children's Hospital, Houston, Texas; [3]Department of Cancer Biology, University of Cincinnati College of Medicine, Cincinnati, Ohio; [4]Department of Neuroscience, Cell Biology and Anatomy, University of Texas Medical Branch, Galveston, Texas; [5]Department of Pediatrics, Texas Children's Cancer Center, Houston, Texas; [6]Department of Pediatrics, Baylor College of Medicine, Houston, Texas; [7]Section of Gastroenterology, Hepatology, and Nutrition, Texas Children's Hospital, Houston, Texas
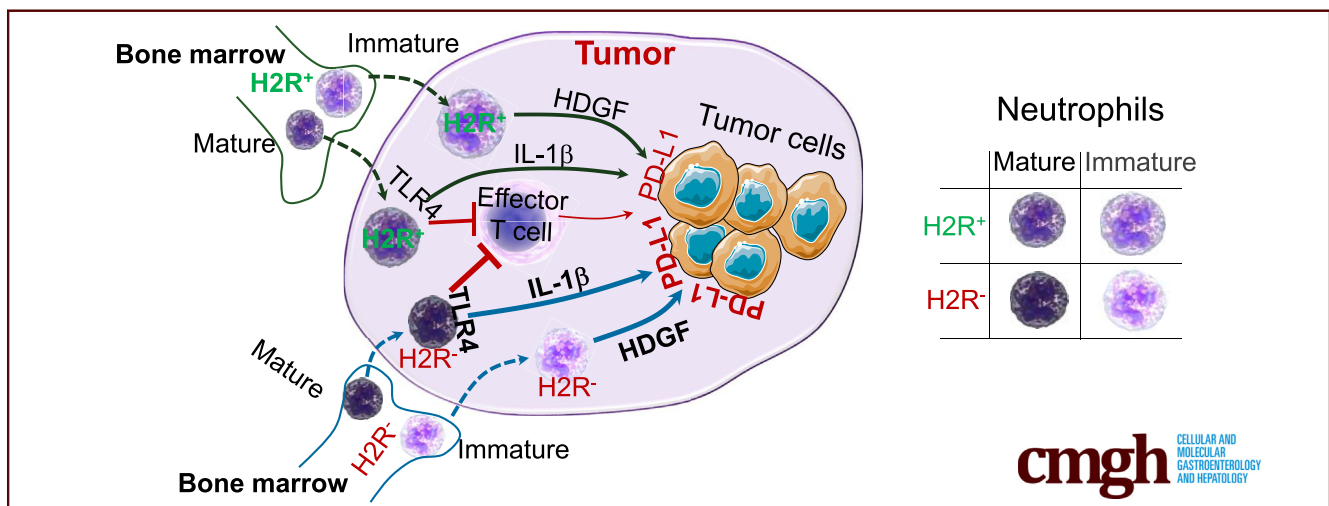
SUMMARY

This study highlights the immunomodulatory role of neutrophil-based histamine type 2–receptor signaling in intestinal inflammation and inflammation-associated colonic tumorigenesis.

BACKGROUND & AIMS: We previously showed that histamine suppressed inflammation-associated colonic tumorigenesis through histamine type 2 receptor (H2R) signaling in mice. This study aimed to precisely elucidate the downstream effects of H2R activation in innate immune cells.

METHODS: Analyses using online databases of single-cell RNA sequencing of intestinal epithelial cells in mice and RNA sequencing of mouse immune cells were performed to determine the relative abundances of 4 histamine receptors among different cell types. Mouse neutrophils, which expressed greater amounts of H2R, were collected from the peritoneum of wild-type and H2R-deficient mice, of which low-density and high-density neutrophils were extracted by centrifugation and

were subjected to RNA sequencing. The effects of H2R activation on neutrophil differentiation and its functions in colitis and inflammation-associated colon tumors were investigated in a mouse model of dextran sulfate sodium–induced colitis.

RESULTS: Data analysis of RNA sequencing and quantitative reverse-transcription polymerase chain reaction showed that *Hrh2* is highly expressed in neutrophils, but barely detectable in intestinal epithelial cells. In mice, the absence of H2R activation promoted infiltration of neutrophils into both sites of inflammation and colonic tumors. H2R-deficient high-density neutrophils yielded proinflammatory features via nuclear factor-κB and mitogen-activated protein kinase signaling pathways, and suppressed T-cell proliferation. On the other hand, low-density neutrophils, which totally lack H2R activation, showed an immature phenotype compared with wild-type low-density neutrophils, with enhanced MYC pathway signaling and reduced expression of the maturation marker Toll-like receptor 4.

CONCLUSIONS: Blocking H2R signaling enhanced proinflammatory responses of mature neutrophils and suppressed neutrophil maturation, leading to accelerated progression of

inflammation-associated colonic tumorigenesis. *(Cell Mol Gastroenterol Hepatol 2022;13:717–737; https://doi.org/10.1016/j.jcmgh.2021.11.003)*

H istamine elicits a variety of physiological processes via activation of histamine receptors (HRs), namely H1R, H2R, H3R, and H4R.[1] We previously showed that histamine suppresses intestinal inflammation and the development of inflammation-associated colon tumors through H2R.[2,3] Consistent with the importance of histamine in cancer development, Yang et al[4] showed that loss of endogenous histamine significantly inhibited neutrophil maturation, resulting in the acceleration of inflammation-associated colon cancer in dextran sulfate sodium (DSS)-treated histidine decarboxylase–deficient mice. However, the detailed effects of H2R downstream signaling on immune cells, inflammation, and cancer remain unclear.

Infiltration of inflammatory immune cells is a common feature in human cancers. Although immune cells, in theory, should respond to tumor development and help control tumor growth, as the tumor develops the cancer cell mechanisms to evade immune cells and promote tolerance. Tumor immune tolerance is driven by the expansion of suppressor-cell populations, including myeloid-derived suppressor cells (MDSCs), which consist of granulocytic MDSCs and monocytic MDSCs that can suppress T-cell functions and promote tumor angiogenesis and metastasis. Of these, granulocytic MDSCs (neutrophils) are the predominant MDSC population in solid tumors and play a critical role in tumor-associated immune suppression.[5] MDSCs inhibit the antitumor T-cell effector phase through various mechanisms, including producing reactive oxygen species (ROS) and arginase-1,[6] reducing cysteine in the environment,[7] up-regulating expression of programmed death-ligand 1 (PD-L1),[8] promoting secretion of Gal-9,[9] and producing S100A8/S100A9 (the endogenous Toll-like receptor [TLR]4 ligands).[10–12] As a result, many research and clinical efforts currently are underway trying to suppress MDSC numbers and function in cancers.

Histamine has been shown to suppress MDSC functions and intratumoral infiltration of MDSCs.[13] However, it is not clear which histamine receptor is responsible for this effect in MDSCs. H2R activation by histamine has been shown to inhibit neutrophil chemotaxis[14] and leukotriene synthesis through adenosine 3′,5′-cyclic monophosphate–dependent protein kinase signaling[15] and to suppress reduced nicotinamide adenine dinucleotide phosphate oxidase activation induced by WKYMVM and N-formyl-methionyl-leucyl-phenylalanine in human neutrophils.[16] Because reduced nicotinamide adenine dinucleotide phosphate oxidase–mediated ROS production is a key factor to suppress T-cell functions, it is reasonable to hypothesize that H2R activation may modulate MDSC functions.

In this study, we show that disruption of H2R signaling enhanced MDSC functions in vitro and significantly aggravated inflammation-associated colonic carcinogenesis in mice. Gene signature analysis showed the mechanisms by which H2R signaling promotes neutrophil maturation during granulopoiesis and suppresses proinflammatory responses in mature neutrophils.

Results

Intestinal *Hrh2 Is Expressed Almost Exclusively in Neutrophils*

We previously reported that histamine may affect the development of inflammation-associated colon cancer through different histamine receptors, H1R and H2R.[3] However, expression of histamine receptors in different cell types has not been thoroughly examined. To address this point, we performed quantitative reverse-transcription polymerase chain reaction (qRT-PCR) to compare mRNA quantities of *Hrh1* and *Hrh2* among mouse macrophages, neutrophils, T cells, and mouse colonic epithelium–derived colonoids. *Hrh1* is expressed in macrophages and colonic epithelial cells, while *Hrh2* is expressed predominantly in neutrophils, but not in intestinal epithelial cells (Figure 1*A*). Taking advantage of available online single-cell RNA sequencing data (available from: singlecell.broadinstitute.org), we confirmed that in mouse intestinal epithelial cells (GEO: GSE92332), less than 0.2% of total cells expressed *Hrh1*, and approximately 3% of enteroendocrine cells expressed *Hrh3*. Intestinal epithelial cells did not harbor *Hrh2* or *Hrh4* beyond negligible quantities (Figure 1*B*). Using another data set of human colonic epithelial cells from patients with ulcerative colitis (UC) and healthy controls (Single Cell Portal accession: SCP259), we observed that approximately 4% of intestinal epithelial cells expressed *HRH1*, while neither *HRH2* or *HRH4* were expressed in any cell type in the intestinal epithelium of healthy individuals. *HRH3* was not included in this study because to its relative absence of expression in human intestinal epithelial cells (Figure 1*C*).

Further analysis of *Hrh2* expression levels in various immune cell types in mice was performed using the Gene Skyline database (available from: http://rstats.immgen.org/Skyline/skyline.html). *Hrh2* was found to be highly expressed in

Figure 1. H2R is highly expressed in neutrophils. (*A*) Relative expression levels of *Hrh1* and *Hrh2* in different cell types of female C57/B6 mice by qRT-PCR (n = 4). (*B*) The gene expression pattern of histamine receptors in mouse intestinal epithelial cells obtained from the single-cell portal (GEO: GSE92332). (*C*) The gene expression pattern of histamine receptors in human intestinal epithelial cells obtained from the single-cell portal (SCP259). (*D*) The relative gene expression of *Hdc*, histamine receptors, and surface markers in different immune cells obtained from the Gene Skyline database (http://rstats.immgen.org/Skyline /skyline.html). (*E*) The gene expression pattern of histamine receptors in human immune cells analyzed using the Human Immune Cell Gene Viewer. mDC, myeloid dendritic cell; mRNA, messenger RNA; NK, Natural killer; PBMC, peripheral blood mononuclear cell; pDC, plasmacytoid dendritic cell; TA, transit amplifying; Th, T helper; Treg, regulatory T cells.

neutrophils isolated from multiple tissues, including bone marrow, spleen, and thioglycolate-stimulated peritoneal cells, while *Hrh1*, *Hrh3*, and *Hrh4* were not expressed in neutrophils (Figure 1*D*). Similar expression patterns of histamine-receptor genes also were observed in human neutrophils (Platform: Human Immune Cell Gene Viewer) (Figure 1*E*), suggesting that histamine signaling may influence neutrophil function through H2R. Increased *Hdc* expression, which promotes histamine production, was observed in neutrophils, suggesting that activation of H2R in neutrophils may be autocrine. It is worth noting that *Hdc* also is expressed in peritoneal macrophages, but at a much lower level compared with that in neutrophils.

H2R Deficiency Aggravated DSS-Induced Colitis and Promoted Inflammation-Associated Dysplasia

Acute colitis was induced in H2R-knockout (H2R KO) and wild-type (WT) control mice by administration of DSS in drinking water. After 1 cycle of 2% DSS for 5 days, H2R-deficient mice showed more severe inflammation compared with the controls (Figure 2*A*). H2R-deficient mice showed disruption of the colonic architecture with increased immune infiltration in the colon. Most colonic crypts remained intact in *Apc^min/+* mice after DSS treatment, with isolated inflammatory lesions in the middle and distal colon. In contrast, the crypt architecture was altered significantly in the middle and distal colon of *Apc^min/+* H2R KO mice, with several notable areas of immune infiltration (Figure 2*A*). These findings were reflected by significantly greater inflammation scores in H2R-deficient mice (4.81 ± 0.36) compared with WT mice (2.53 ± 0.33) (Figure 2*B*). In addition to epithelial disruption, we observed increased numbers of infiltrating neutrophils (S100A8 positive) in H2R-deficient mice (Figure 2*C*).

Intestinal dysplasia may lead to sporadic colorectal cancer (CRC) and inflammation-associated colon cancer in patients with inflammatory bowel disease.[17,18] When treated with 2 cycles of DSS, WT mice harbored 1–2 hyperplastic lesions from the middle to distal colon, but crypt architecture was kept intact with well-differentiated goblet cells (Mucin 2 [MUC2] positive, red). When H2R-deficient mice were treated with 2 cycles of DSS, mice showed more than 3–4 dysplastic lesions consisting of relatively large numbers of proliferating cells (proliferating cell nuclear antigen [PCNA] positive, green) and few goblet cells (Figure 2*D*). Squamous metaplasia (SM) in colorectal polyps has been reported as a precursor lesion of primary colorectal squamous cell carcinoma or colorectal adenocarcinoma with squamous components.[19] Interestingly, all H2R-deficient mice developed SM (7 of 7 mice) in the distal colon after 2-cycle DSS treatment. In contrast, no WT mice developed SM (Figure 2*E*). Notably, proliferating squamous cells (PCNA-positive) were surrounded by neutrophils (S100A8 positive) in the SM lesion (Figure 2*F*, highlighted with white arrows). These findings suggest that neutrophils might promote squamous metaplasia when H2R is deactivated.

H2R Deficiency Promoted Development of Inflammation-Associated Colon Cancer

To evaluate H2R functions in cancer development, we crossed H2R KO and *Apc^Min/+* mice to generate double-mutant mice. Using DSS treatment of *Apc^Min/+* mice, a widely used model to examine inflammation-associated colon cancer,[20,21] we observed multiple tumors in the middle and distal colon of *Apc^Min/+* mice by colonoscopy after 2 cycles of DSS treatment (Figure 3*A*). We observed larger and more abundant tumors in H2R KO/*Apc^Min/+* double-mutant mice compared with WT *Apc^Min/+* mice (Figure 3*A*). Further examination under a dissecting microscope showed greater numbers of colonic tumors in double-mutant mice (19.43 ± 1.59 tumors/mouse) compared with control mice (5.71 ± 0.52 tumors/mouse) (Figure 3*B*), as well as increased tumor size (Figure 3*C*), suggesting that H2R signaling suppresses both tumorigenesis and tumor growth in chronic inflammation. Moreover, neutrophil infiltration was increased in colonic tumors from H2R KO/*Apc^Min/+* mice compared with *Apc^Min/+* control mice (Figure 3*D* and *E*).

Cancer cells commonly evade the immune system by aberrantly expressing the protein PD-L1. PD-L1 suppresses the adaptive immune system and promotes a worse outcome for many cancers. Increased neutrophil numbers are associated positively with PD-L1 expression in CRC.[22] In *Apc^Min/+* control mice, PD-L1 was rarely expressed in the colonic tumor cells, with a rate of 12.5% (1 of 8 mice). In *Apc^Min/+* mice lacking H2R, PD-L1 expression was detected in approximately 90% (7 of 8) of colonic tumors (Figure 3*F* and *G*). Interestingly, neutrophils were found around tumor cells (red signals) where PD-L1 was expressed (Figure 3*H*). Tumor-associated PD-L1 expression might be related to increased numbers of H2R-deficient neutrophils in the local tumor environment.

The acquisition of invasive properties by tumor cells is a key event during tumor development. Immunofluorescence with proliferating tumor cells (PCNA in red) and smooth muscle cells (smooth muscle actin [SMA] in green) showed that colon tumor cells invaded into submucosa in more than 70% of the H2R KO/*Apc^Min/+* mice (7 of 9), whereas no tumors in the *Apc^Min/+* control mice showed such invasive lesions (Figure 3*I* and *J*). These findings show that H2R signaling in mucosal neutrophils may suppress tumor cell invasion.

RNA Sequencing Showed Distinct Gene Signatures for Low- and High-Density Neutrophils

Neutrophils can be separated into high-density and low-density fractions by density gradient centrifugation. Most high-density cells are mature granulated neutrophils (high-density neutrophils [HDNs]), whereas low-density neutrophils (LDNs) are immature granulated neutrophils and mature degranulated neutrophils.[23] We first separated casein-elicited mouse peritoneal cells into HDNs and low-density cells, and then further purified LDNs within the low-density cells using a negative selection kit (Figure 4*A*).
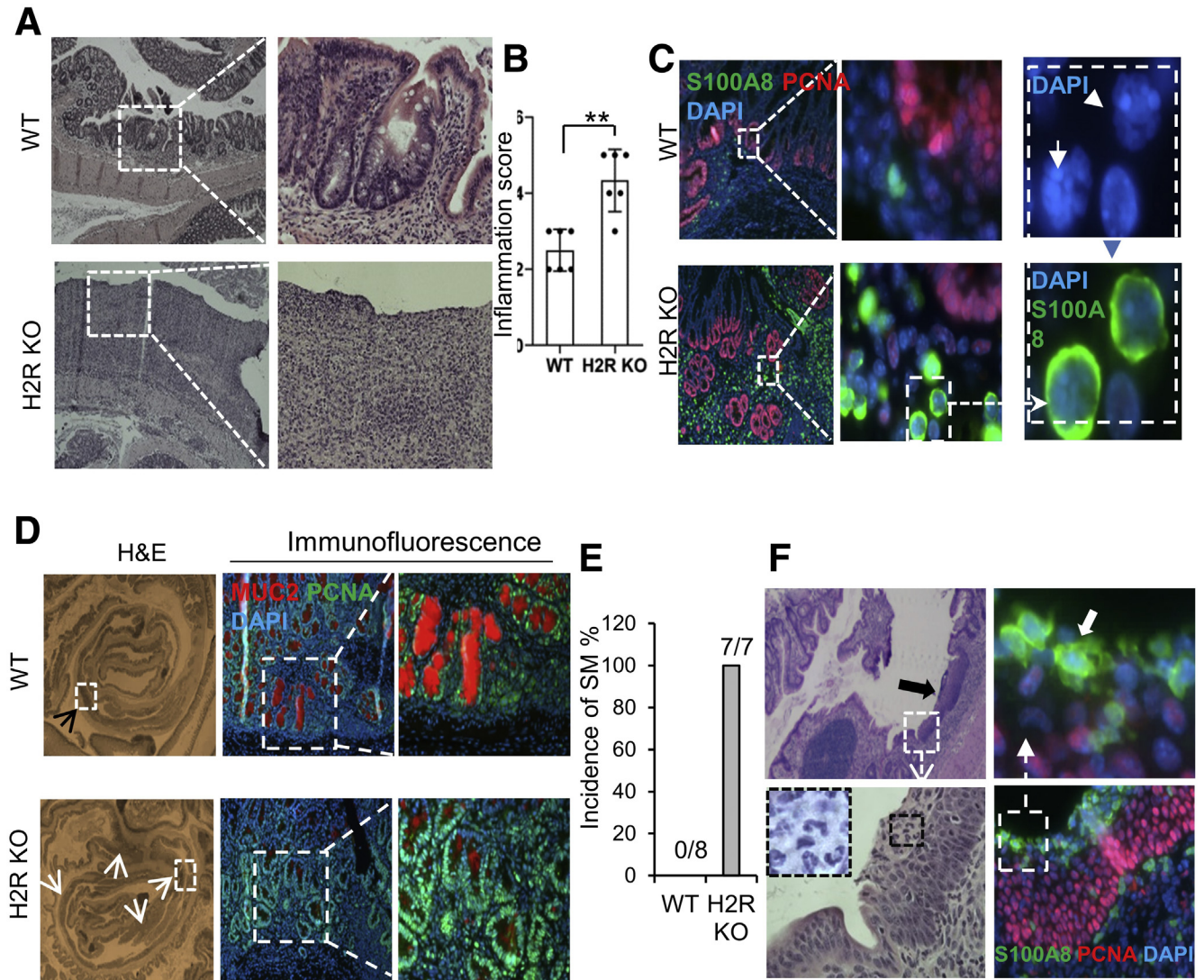
Figure 2. *H2R* inactivation in mice resulted in aggravated DSS-induced colitis. (*A*) H&E staining (magnification: 40× and 200×) of middle and distal colon of WT and H2R-deficient mice after DSS treatment. Crypt polarity and architecture were disrupted in the middle and distal colon of H2R-deficient mice. (*B*) Inflammation scores were calculated based on the epithelial damage and infiltrating inflammatory cells from proximal to distal colon in 3 H&E sections from each mouse (total, 6 pairs of mice). Values are means ± SD. **$P < .01$. (*C*) Immunofluorescence (magnification: 40×, 200×, and 1000×) of S100A8 (green), proliferating cell nuclear antigen (PCNA) (red), and 4′,6-diamidino-2-phenylindole (DAPI) (blue, nuclear DNA staining) in the DSS-treated colon in WT and H2R KO mice. (*D*) DSS-induced hyperplasia (*top*, indicated by a *black arrowhead*) and dysplasia (*bottom*, indicated by *white arrowheads*) (magnification: 40×) in the colons of WT and H2R KO mice, respectively. Immunofluorescence (magnification: 200× and 400×) of MUC2 (red) and PCNA (green) shows much fewer MUC2-positive mature goblet cells in the DSS-treated colon of H2R KO mice. (*E*) The incidence of squamous metaplasia of DSS-treated WT (n = 8) and H2R KO (n = 7) mice. (*F*) H&E staining (magnification: 40× and 200×) and immunofluorescence (magnification: 200× and 1000×) of S100A8 (green, indicated by a white arrow) and PCNA (red) for the DSS-induced SM lesions (indicated by a *black arrow*) in the distal colon in H2R KO mice.

The purity for HDNs and LDNs (CD11b$^+$Ly6g$^+$) was determined to be 98% and 92%, respectively, by flow cytometry (Figure 4*B*). We performed RNA sequencing on HDN and LDN cells from both WT and H2R-deficient mice (GSE162850). RNA sequencing identified 941 up-regulated genes in WT HDN populations (*P*adjusted < .05; average fold change, >1.4) (Figure 4*C*), and 800 up-regulated genes in WT LDN populations (*P*adjusted < .05; average fold change, >1.6). To fully explore the gene signature of the whole transcriptome, especially to capture low-amplified genes that may be below the signal-to-noise significance cut-off level, we applied unbiased Gene Set Enrichment Analysis using whole HDNs and LDN transcriptome. At a conventional threshold of $P < .05$ and a false-discovery rate

of less than 0.25, 8 and 11 pathways were enriched significantly in LDNs and HDNs, respectively. We found that LDNs harbor enriched immature/pro-proliferative pathways, such as increased expression of MYC pathways, E2F targets, and

G2M checkpoints (Figure 4D). Figure 4E and F show the enriched gene map and gene list of MYC targets, respectively. On the contrary, HDNs showed mature/proinflammatory features, such as increased expression of the
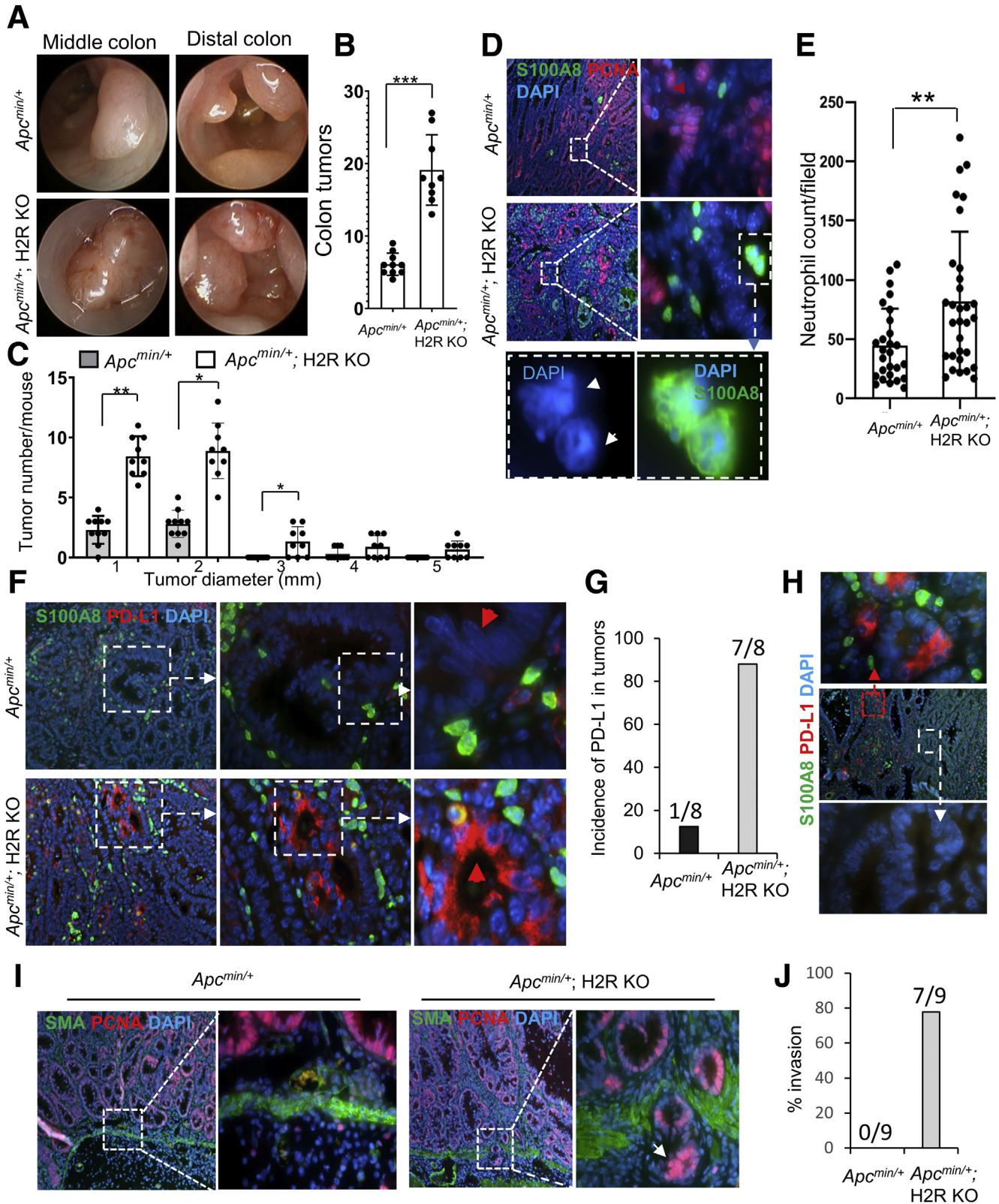
genes involved in tumor necrosis factor (TNF) signaling via the nuclear factor-κB (NF-κB) pathway, interferon-γ pathway, and the interleukin (IL)6 Janus kinase signal transducer and activator of transcription pathway (Figure 4G). As an example, enrichment of TNF signaling via the NF-κB pathway and the corresponding gene lists are shown in Figure 4H and I. The relative expression levels of representative genes for MYC targets, NF-κB pathway, and surface markers were verified by qRT-PCR (Figure 5A–C). These unique gene signatures of mouse HDNs and LDNs showed the distinct functions of mature and immature neutrophils.

CXCR2 and TLR4 are known to be neutrophil differentiation markers.[24] We performed immunofluorescence for S100A8, CXCR2, and TLR4 on HDNs and LDNs. As expected, most HDNs showed positive staining for both CXCR2 and TLR4, confirming their mature features. However, in some LDNs, low CXCR2 expression was detected with no detectable level of TLR4 (Figure 5D). Therefore, TLR4 should be used as a maturation marker rather than as a differentiation marker. In our RNA sequencing data, we also observed greater expression of the endogenous ligands for TLR4 S100a8 and S100a9 in HDNs than in LDNs (Figure 5E), suggesting that HDNs harbor more proinflammatory features.

H2R Deficiency Inhibited Neutrophil Maturation

Ly6G and CD11b are early neutrophil markers, expressed even in the promyelocyte stage.[24] Flow cytometry analysis did not show a significant difference in the CD11b+Ly6G+ cell population between H2R KO and WT cells from bone marrow and in blood (Figure 6A), indicating that H2R deficiency did not affect the initial neutrophil lineage commitment. We next sought to determine whether H2R signaling was involved in neutrophil maturation. RNA sequencing showed 929 down-regulated genes (Padjusted < .05; average fold change, >1.4) and 496 up-regulated genes (Padjusted < .05; average fold change, >1.4) in H2R KO LDNs compared with WT LDNs. The top genes of each group are shown in the heatmap (Figure 6B). Strikingly, loss of H2R, confirmed by exon use (Figure 6C), in LDNs further enhanced the gene expression of pro-proliferative pathways, such as the MYC and E2F target pathways (Figure 6D). The enrichment map of MYC targets and the corresponding gene list are included in Figure 6E and F, respectively.

Interestingly, WT LDNs expressed relatively greater levels of inflammatory pathway genes than H2R-deficient LDNs (Figure 6G). The enrichment map of inflammatory response and inflammatory pathway gene list indicated a proinflammatory phenotype of WT LDNs (Figure 6H and I). In H2R KO LDNs, we observed increased expression of MYC targets (Figure 6J), and decreased levels of prodifferentiation transcription factors, such as CCAAT/enhancer-binding protein (CEBP) family members (Figure 6K). We also found reduced cell surface markers, such as Cxcr2, Tlr4, and Itgam (Figure 6L), and increased quantities of growth factors such as Hdgf (Figure 6M) in H2R KO LDNs compared with WT LDNs. These findings suggest that H2R signaling plays a central role during neutrophil maturation. Based on our RNA sequencing data, we speculate that H2R activation suppresses pro-proliferative signals, such as MYC and MYC targets, thereby promoting cell maturation.

Our data identified that Hrh2 expression was correlated negatively with Myc expression in neutrophils. Moreover, a negative correlation was found between expression of Hrh2 and Myc in a spectrum of mouse and human immune cells (Figure 7A and B). This phenomenon also was found in pathologic settings, such as in leukocytes in pneumonia (Figure 7C) and in acute myeloid leukemia (Figure 7D). In fact, increased TCF4 gene expression, an important transcription factor of MYC, was shown in the H2R KO LDNs compared with WT LDNs by RNA sequencing (Figure 7E). We therefore speculate that H2R signaling might suppress MYC expression.

All neutrophils, both mature and immature, originate from bone marrow. By S100A8, TLR4 and CXCR2 staining, we found more TLR4-negative neutrophils in the bone marrow of H2R-deficient mice (Figure 8A and B), consistent with our pathway and gene expression data. Cell-cycle analysis showed a significant increase in S-phase cells and a decrease in G_0/G_1-phase cells in H2R-deficient bone marrow compared with WT bone marrow (Figure 8C), suggesting that H2R signaling activation may suppress cell proliferation. H2R-deficient mice showed similar pathologic phenotypes during colitis, as previously shown in Hdc knockout mice. Consistent with the results using H2R-deficient neutrophils, histidine decarboxylase deficiency also resulted in increased Myc expression in both HDNs and LDNs (Figure 8D). These findings suggest that histamine suppresses Myc expression and promotes neutrophil maturation through H2R signaling.

Figure 3. (*See previous page*). **H2R deficiency promoted the development of inflammation-associated colon cancer in Apc$^{min/+}$ mice.** (*A*) Representative images taken during colonoscopy of mice at the end of the second recovery phase. (*B* and *C*) Tumor numbers were counted and measured in the entire colon of Apc$^{min/+}$ (n = 10) and Apc$^{min/+}$; H2R KO (n = 9) mice under a dissecting microscope. (*D*) Infiltrating neutrophils stained with S100A8 antibody (green) (magnification: 40×, 200×, and 1000×). (*E*) The mean numbers of neutrophils in 8 fields at 200× power for each Apc$^{min/+}$ (n = 4) and each Apc$^{min/+}$; H2R KO (n = 4) mouse. (*F*) Immunofluorescence of S100A8 (green) and PD-L1 (red) for colon tumors (magnification: 40×, 200×, and 400×). The *red arrowhead* in the *top* panel indicates the Apc$^{min/+}$ tumor cells that do not express PD-L1, and the *red arrow* in the bottom panel indicates the tumor cells that express PD-L1 in Apc$^{min/+}$; H2R KO mice. (*G*) Incidence of PD-L1–positive tumors for Apc$^{min/+}$ (n = 8) and Apc$^{min/+}$; H2R KO (n = 8) mice. (*H*) Immunofluorescence (magnification: 40× and 200×) of S100A8 (green) and PD-L1 (red) for Apc$^{min/+}$; H2R KO tumors. (*I*) Immunofluorescence (magnification: 40× and 200×) of proliferating cell nuclear antigen (PCNA) (red) and smooth muscle actin (SMA) (green). The *arrow* indicates invading tumor cells through the muscularis mucosae into the submucosa. (*J*) Percentage of invasion in tumors of Apc$^{min/+}$ (n = 9) and Apc$^{min/+}$; H2R KO (n = 9) mice. In all panels, means ± SD are shown. **P < .01 and ***P < .001. DAPI, 4′,6-diamidino-2-phenylindole.
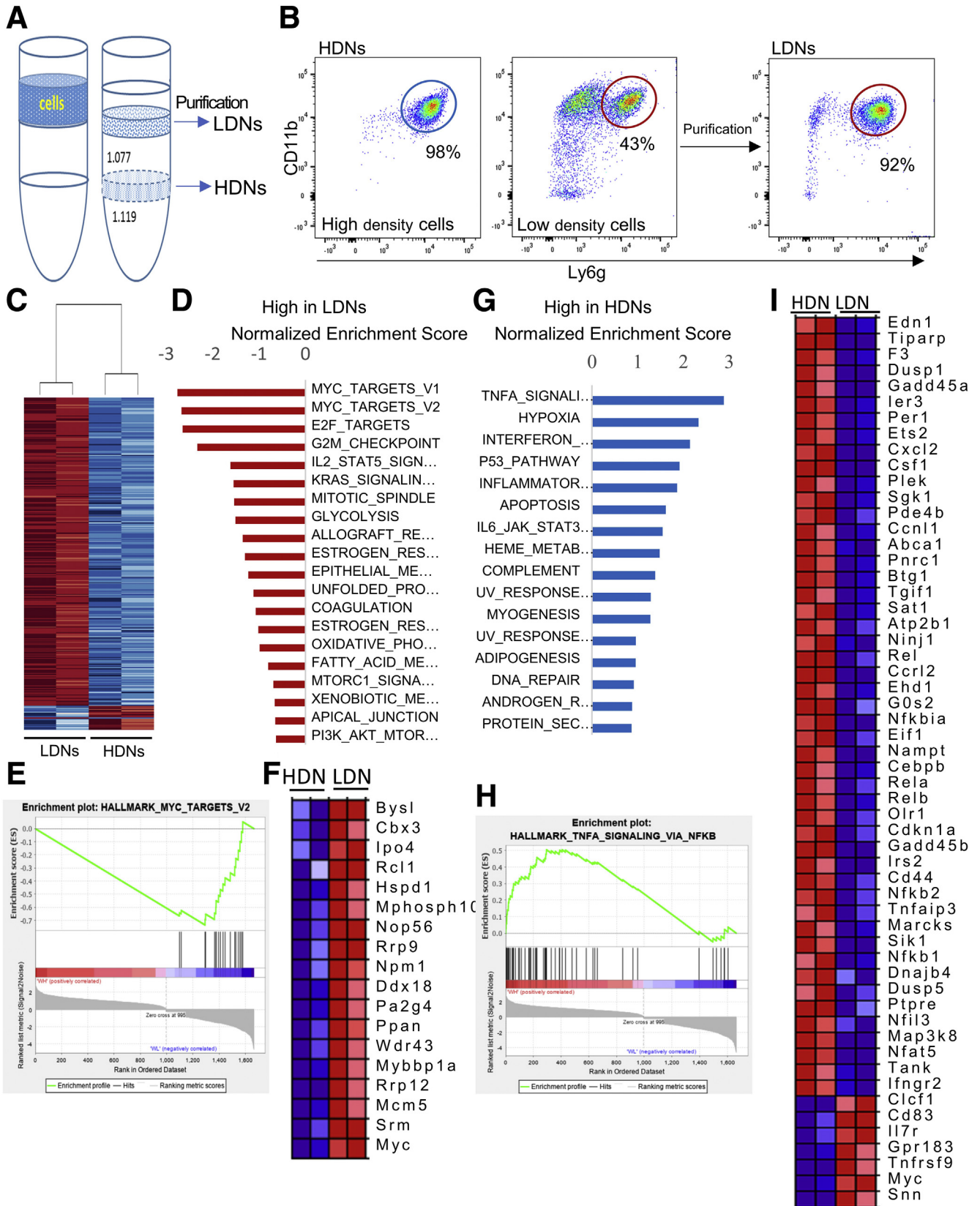
Figure 4. The distinct gene signatures of LDNs and HDNs. (*A*) Schematic illustration showing how LDNs and HDNs are isolated from peritoneal cells. (*B*) The purity of HDNs and purified LDNs was determined by flow cytometry using CD11b and Ly6g antibodies. (*C*) The heat map of representative genes of LDNs and HDNs. (*D*) Identification of the top pathways enriched in LDNs were assessed by gene set enrichment analysis with Hallmark gene sets (h.all.v7.1.symbols). (*E* and *F*) The enrichment plot and gene list of MYC targets in HDNs and LDNs. (*G*) Identification of the top pathways enriched in HDNs were assessed by gene set enrichment analysis with Hallmark gene sets. (*H* and *I*) The enrichment plot (*H*) and enriched genes (*I*) of TNFα signaling pathway via NF-κB. WH, WT high-density ; WL, WT low-density.
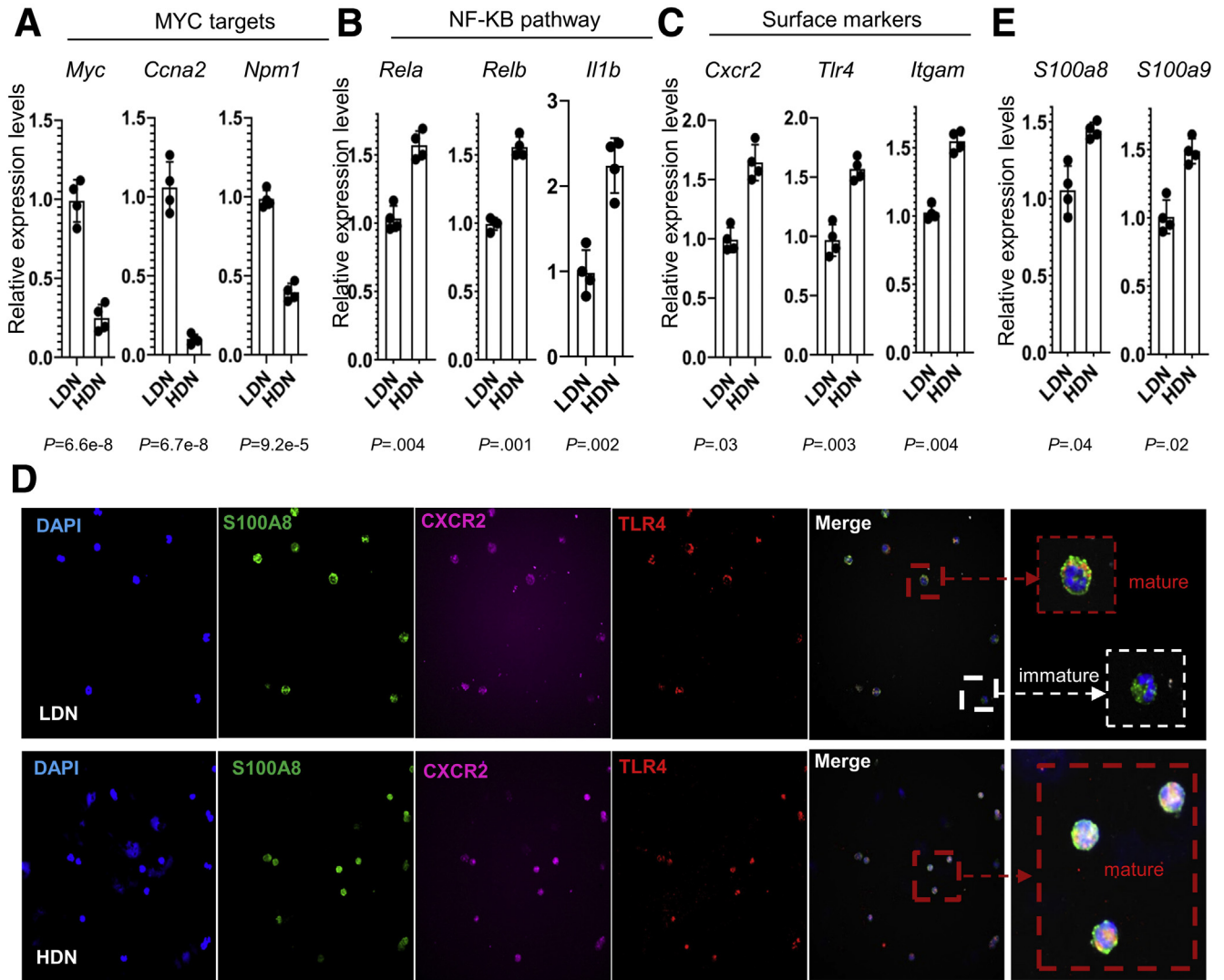
Figure 5. Confirmation of the distinct gene signatures of LDNs and HDNs. (*A–C*) Expression of representative genes in MYC target, NF-κB pathways, and surface markers of LDNs and HDNs by qRT-PCR (n = 4). Means $\pm$ SD are shown. The *P* value is shown under each panel. (*D*) Immunofluorescence staining (magnification: 200$\times$ and 1000$\times$) of S100A8 (green), CXCR2 (pink), and TLR4 (red) in LDNs and HDNs. (*E*) The expression levels of *S100a8* and *S100a9* in LDNs and HDNs by qRT-PCR (n = 4). Means $\pm$ SD are shown. *P* values are shown on the panel. CXCR2, C-X-C Motif Chemokine Receptor 2; DAPI, 4′,6-diamidino-2-phenylindole.

H2R Signaling Modulated Neutrophil Chemotaxis and Mitogen-Activated Protein Kinase Signaling
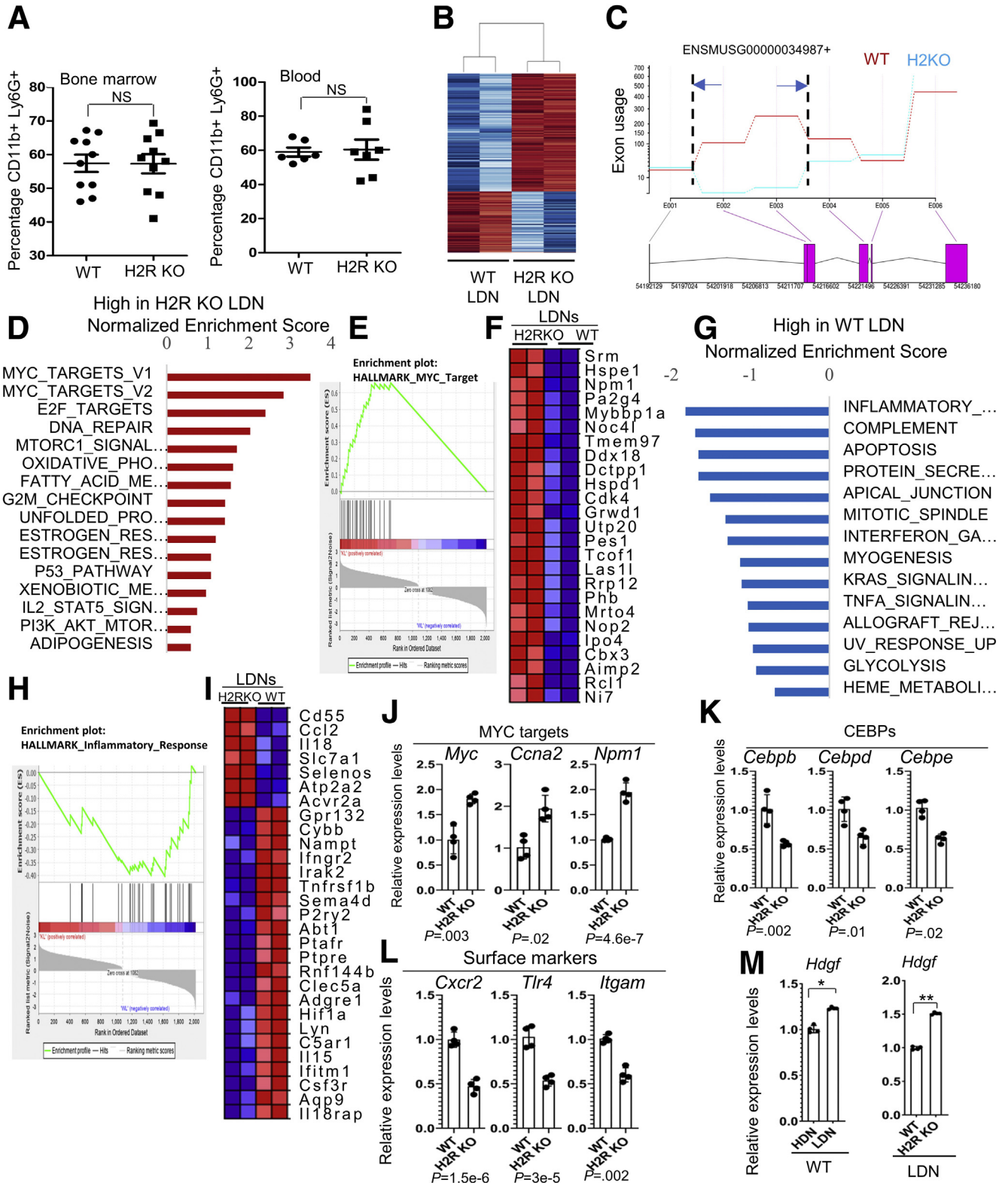
As first responders during infection, neutrophils can be activated by different pathogen-associated molecular patterns through multiple highly expressed Toll-like receptors. Activation of pathogen-associated molecular patterns triggers downstream pathways, such as NF-κB and mitogen-activated protein kinase (MAPK) pathways, to induce proinflammatory cytokine production. The activation of NF-κB signaling and MAPKs in response to lipopolysaccharide (LPS) stimulation in neutrophils was determined by Western blot, using antibodies against phosphorylated inhibitor of nuclear factor-κB (iκB), phosphorylated extracellular signal-regulated kinase (ERK), and phosphorylated p38 MAPK. LPS treatment strongly 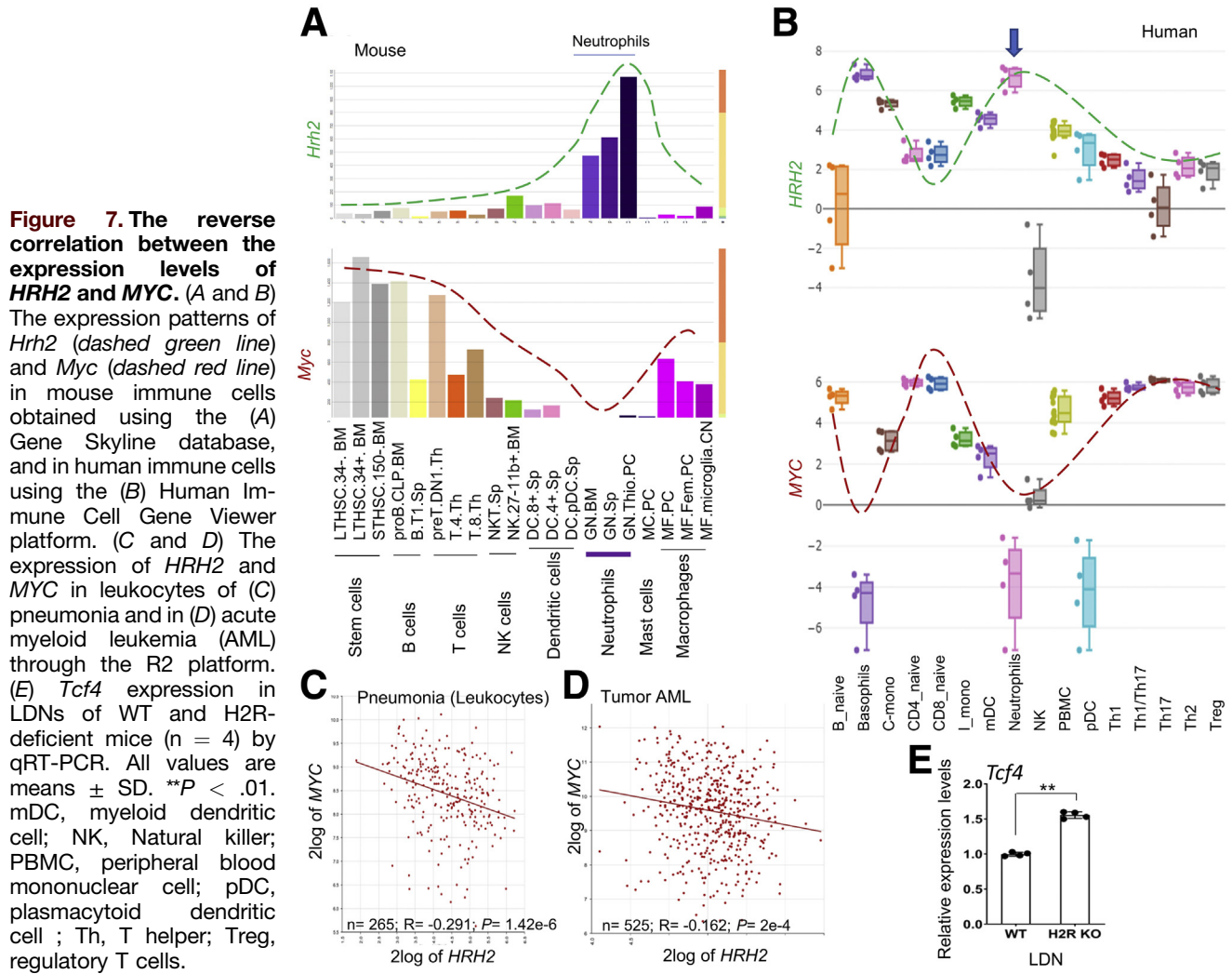induced the activation of NF-κB in H2R-deficient HDNs compared with control HDNs. On the other hand, LPS induced NF-κB activation in control LDNs, but not in H2R-deficient LDNs (Figure 9*A*), suggesting that H2R activation suppresses NF-κB signaling in mature and immature neutrophils during inflammation or cancer.

We previously showed that H2R activation suppresses phosphorylation of ERK and p38 in macrophages and colorectal cancer cells.[3] Consistent with these findings, we found enhanced ERK phosphorylation in H2R-deficient neutrophils compared with WT neutrophils without LPS stimulation. Moreover, LPS treatment induced stronger p38 activation in H2R-deficient neutrophils than in the WT neutrophils, especially in HDNs (Figure 9*A*). The activation of these key proinflammatory pathways could explain more severe intestinal inflammation in H2R-deficient mice.

Consequently, MagPix (Luminex Corporation) was used to analyze the production of cytokines induced by LPS in HDNs and LDNs. The relative concentrations of IL1α, IL1β, IL6, IL10, and TNF were increased significantly after LPS treatment for 6 hours in the H2R-deficient HDNs than in control HDNs (Figure 9B). However, this phenotype was not observed in H2R-deficient LDNs (Figure 9C). We speculate that this result may be owing to reduced TLR4 expression in H2R KO LDNs compared with control LDNs. Increased amounts of IL1β also were found in neutrophils in mucosal inflammation (Figure 9D), as well as in colonic tumors (Figure 9E). In addition to IL1β protein, an increase in the

Figure 7. **The reverse correlation between the expression levels of HRH2 and MYC.** (A and B) The expression patterns of Hrh2 (*dashed green line*) and Myc (*dashed red line*) in mouse immune cells obtained using the (A) Gene Skyline database, and in human immune cells using the (B) Human Immune Cell Gene Viewer platform. (C and D) The expression of HRH2 and MYC in leukocytes of (C) pneumonia and in (D) acute myeloid leukemia (AML) through the R2 platform. (E) Tcf4 expression in LDNs of WT and H2R-deficient mice (n = 4) by qRT-PCR. All values are means ± SD. **P < .01. mDC, myeloid dendritic cell; NK, Natural killer; PBMC, peripheral blood mononuclear cell; pDC, plasmacytoid dendritic cell ; Th, T helper; Treg, regulatory T cells.

expression of IL1β receptor 1 gene *Il1r1* was observed in tumor samples (Figure 9F), suggesting that the IL1 pathway could be more potently activated in H2R-deficient mice. In human colorectal cancer, increased *IL1R1* expression was associated with significantly worse outcomes (Figure 9G), suggesting the potential involvement of the IL1 pathway in the pathogenesis of colon cancer.

LPS also has been shown to induce Programmed death ligand 1 (PD-L1) expression in human polymorphonuclear leukocyte.[8] We found that LPS treatment promoted *CD274* (PD-L1 gene) expression in all neutrophils, especially in LDNs by qRT-PCR (Figure 10A). This finding suggests that

neutrophils might directly suppress T-cell proliferation through the PD-L1/PD1 axis. Next, we evaluated the suppressive effects of HDNs and LDNs on CD8$^+$ T-cell proliferation in vitro. Similar to other studies,[6] we found that HDNs, the mature neutrophils, can suppress CD8+ T-cell proliferation (Figure 10B). Interestingly, LDNs were not found to suppress T-cell proliferation. One of the mechanisms MDSCs use to suppress T-cell function is through generation of ROS.[25] We found that the H2R-deficient HDNs enhanced suppression of T-cell proliferation compared with the WT HDNs (Figure 10C); however, this effect was not modified by the addition of a ROS scavenger, N-

---

Figure 6. (*See previous page*). **H2R deficiency altered features of LDNs.** (A) Neutrophil populations (CD11b+ Ly6g+) in bone marrow (n = 10) and in blood (n = 7) of WT and H2R-deficient mice. (B) A heat map of representative genes of WT and H2R-deficient LDNs. (C) The confirmation of HRH2 gene deletion (exons 2 and 3) by exon use by RNA sequencing. (D) Identification of the top pathways that are enriched most significantly in H2R KO LDNs were assessed by gene set enrichment analysis using Hallmark gene sets. (E and F) The enrichment plot and gene list of MYC targets in WT and H2R-deficient LDNs. (G) Identification of the top pathways that are enriched most significantly in WT LDNs were assessed by gene set enrichment analysis using Hallmark gene sets. (H and I) The enrichment plot and gene list of the inflammatory response pathway in WT and H2R-deficient LDNs. (J–L) The expression of representative genes in MYC target, CEBP family members, and surface markers of WT and H2R-deficient LDNs by qRT-PCR (n = 4). (M) Hdgf expression in HDNs and LDNs of WT and H2R-deficient mice (n = 4) by qRT-PCR. All values are means ± SD. *P < .05, **P < .01, and ***P < .001. CEBP, CCAAT/enhancer binding protein; KL, Knockout low-density; WL, WT low-density.
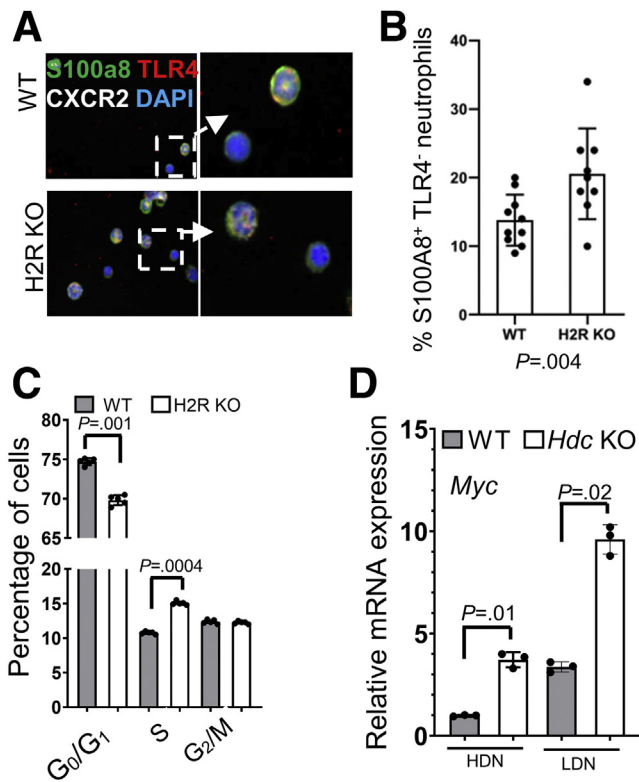
Figure 8. H2R deficiency promoted DNA synthesis in bone marrow cells. (*A*) Immunofluorescence staining (magnification: 200× and 1000×) of S100A8 (green), CXCR2 (white), and TLR4 (red) in WT and H2R-deficient bone marrow cells. (*B*) The mean numbers in each field of TLR4-negative neutrophils at 400× power (n = 10). (*C*) DNA content of different phases of bone marrow cells determined by flow cytometry (n = 5). (*D*) The expression levels of *Myc* in HDNs and LDNs of WT and *Hdc* KO mice by qRT-PCR (n = 3). In all panels, means ± SD are shown. The *P* value is shown in each panel. CXCR2, C-X-C Motif Chemokine Receptor 2; DAPI, 4′,6-diamidino-2-phenylindole; mRNA, messenger RNA.

acetylcysteine. These findings suggest that H2R-deficient HDN-mediated T-cell suppression is independent of ROS production. In contrast to N-acetylcysteine, T-cell suppression by H2R-deficient HDNs was enhanced significantly by adding N-formylmethionyl-leucyl-phenylalanine (fMLP), a compound that activates neutrophils (Figure 10*D*). It has been shown that histamine inhibits neutrophil mobility via H2R signaling.[26] We observed that H2R deficiency promoted random migration, as well as fMLP-mediated chemotaxis, in both HDNs and LDNs (Figure 10*E*). This is in line with the in vivo phenotype, in that more neutrophils infiltrated the areas of intestinal inflammation and colonic tumors.

H2R Antagonism Suppressed Neutrophil Maturation and Promoted Inflammation-Associated Colon Cancer

Finally, we tested whether an H2R antagonist, cimetidine, also could aggravate colonic inflammation and promote colon tumor development. Compared with control

neutrophils, LDNs from cimetidine-treated mice showed significantly increased levels of expression of MYC target genes, and reduced expression of surface markers, including *Tlr4*, *Cxcr2*, and *Itgam* (Figure 11*A*–*C*). Furthermore, an increase in the S phase and a decrease in the G0/G1 phase of bone marrow cells also were observed in cimetidine-treated mice (Figure 11*D*), suggesting that inhibition of H2R by cimetidine promotes cell proliferation in the bone marrow. In cimetidine-treated mice, more and larger tumors were visualized by colonoscopy and direct macroscopic observation compared with WT controls (Figure 11*E* and *F*). Consistent with the results of the H2R-deficient mice, most cimetidine-treated mice developed squamous metaplasia in the distal colon during DSS-induced chronic inflammation, which was not observed in the control mice (Figure 11*G* and *H*).

Importantly, cimetidine treatment promoted PD-L1 expression in the DSS-induced colon tumors in *Apc^Min/+* mice (Figure 11*I* and *J*), which is consistent with the phenotypes found in H2R-deficient mice. In line with the preceding in vitro results, cimetidine significantly enhanced the suppression of CD8$^+$ T-cell proliferation by HDNs (Figure 11*K*). Collectively, our data showed that absence of H2R signaling shifts gene expression patterns of neutrophils toward creating a proinflammatory and protumorigenic microenvironment in the colon (Figure 12).

Discussion

Herein, we showed that H2R is highly expressed in neutrophils, and disruption of H2R signaling, either by genetic manipulation or by antagonists such as cimetidine, influences the maturation stage-specific features of neutrophils. Our study showed that H2R-deficient mature neutrophils harbored more proinflammatory features, which promoted increased colonic cancer pathophysiology. We also found that H2R-deficient immature neutrophils expressed growth factor–related genes, indicating a proproliferative phenotype. Our data indicate that H2R-inactivated neutrophils create a tumor-friendly microenvironment that may accelerate tumor development in mice. Our study details the role of H2R signaling in neutrophils and downstream consequences for inflammation-associated colon cancer development.

Physiologically, neutrophil homeostasis is strictly maintained from granulopoiesis (release from the storage in the bone marrow) to migration into peripheral blood and tissues.[27] In the setting of inflammation or cancer, neutrophils are released from the bone marrow before full maturation, which is enhanced by a loss of endogenous histamine.[4] Our study showed that histamine signaling is involved in neutrophil maturation and contributes to the central role of neutrophils in innate immunity. Inactivation of H2R resulted in significant changes in the relative expression of genes involved in multiple pathways (eg, MYC and E2F) in neutrophils. Our data indicate that H2R activation may suppress proliferation of immature neutrophils. Our results are consistent with recent reports showing that H2R activation is required to promote quiescence of myeloid-biased
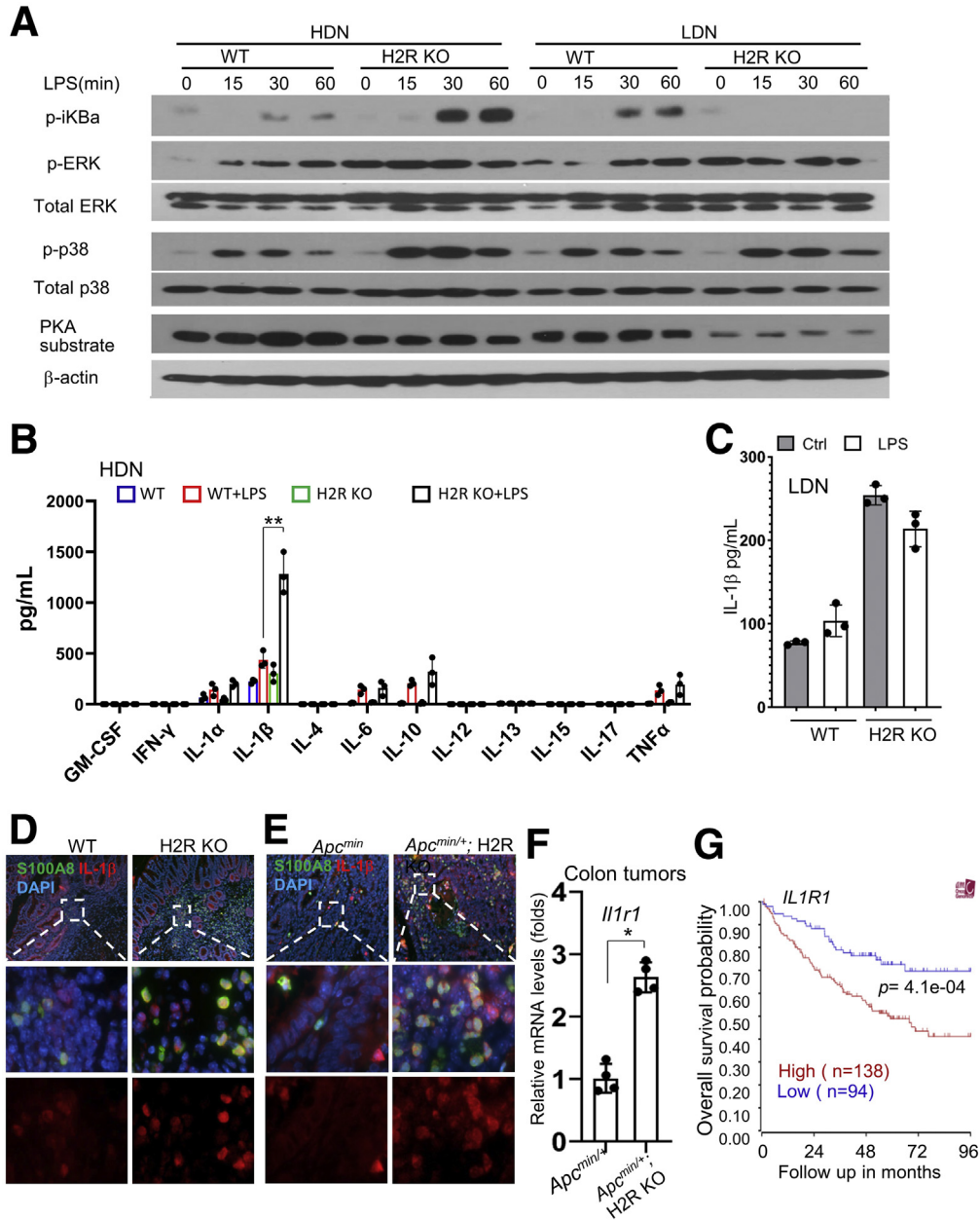
Figure 9. H2R deficiency activated the IL1 signaling pathway. (*A*) Western blot of HDNs and LDNs treated with LPS using antibodies against p-iκBa, p-ERK, total ERK, p-p38, total p38, adenosine 3′,5′-cyclic monophosphate–dependent protein kinase (PKA) substrate, and γ-actin. (*B*) The cytokine production of WT and H2R KO HDNs treated with LPS by MagPix (n = 3). (*C*) IL1β production in WT and H2R KO LDNs treated with LPS (100 ng/mL) by MagPix (n = 3). (*D* and *E*) Immunofluorescence staining of S100A8 and IL1β for (*D*) inflammation and for (*E*) inflammation-associated colon tumors (magnification: 40× and 400×). (*F*) The expression levels of *Il1r1* in the colon tumors of *Apc*$^{Min/+}$ and *Apc*$^{Min/+}$; H2R KO mice by qRT-PCR (n = 4). Means ± SD are shown. *P < .05. (*G*) The association between *IL1R1* expression in cancers and overall survival in CRC patients through the R2 database. Ctrl, control; DAPI, 4′,6-diamidino-2-phenylindole; GM-CSF, Granulocyte macrophage-colony stimulating factor; IFN, interferon.

hematopoietic stem cells (HSCs).[28] Considering that MYC is not expressed in the quiescent HSCs,[29] we believe that H2R activation contributes to the maintenance of the quiescent status of HSCs through suppressing MYC expression. Moreover, immature neutrophils lacking H2R activation secrete more pro-proliferative factors, including hepatoma-derived growth factor (HDGF), into the environment. Cancer cell–derived HDGF has been shown recently to promote carcinogenesis of colorectal cancer.[30] We therefore speculate that release of HDGF from neutrophils may promote neighboring tumor cells to proliferate in a paracrine manner, creating an environment conducive to tumor proliferation. Conversely, increased H2R gene expression may result in tumor growth by suppressing MYC gene expression
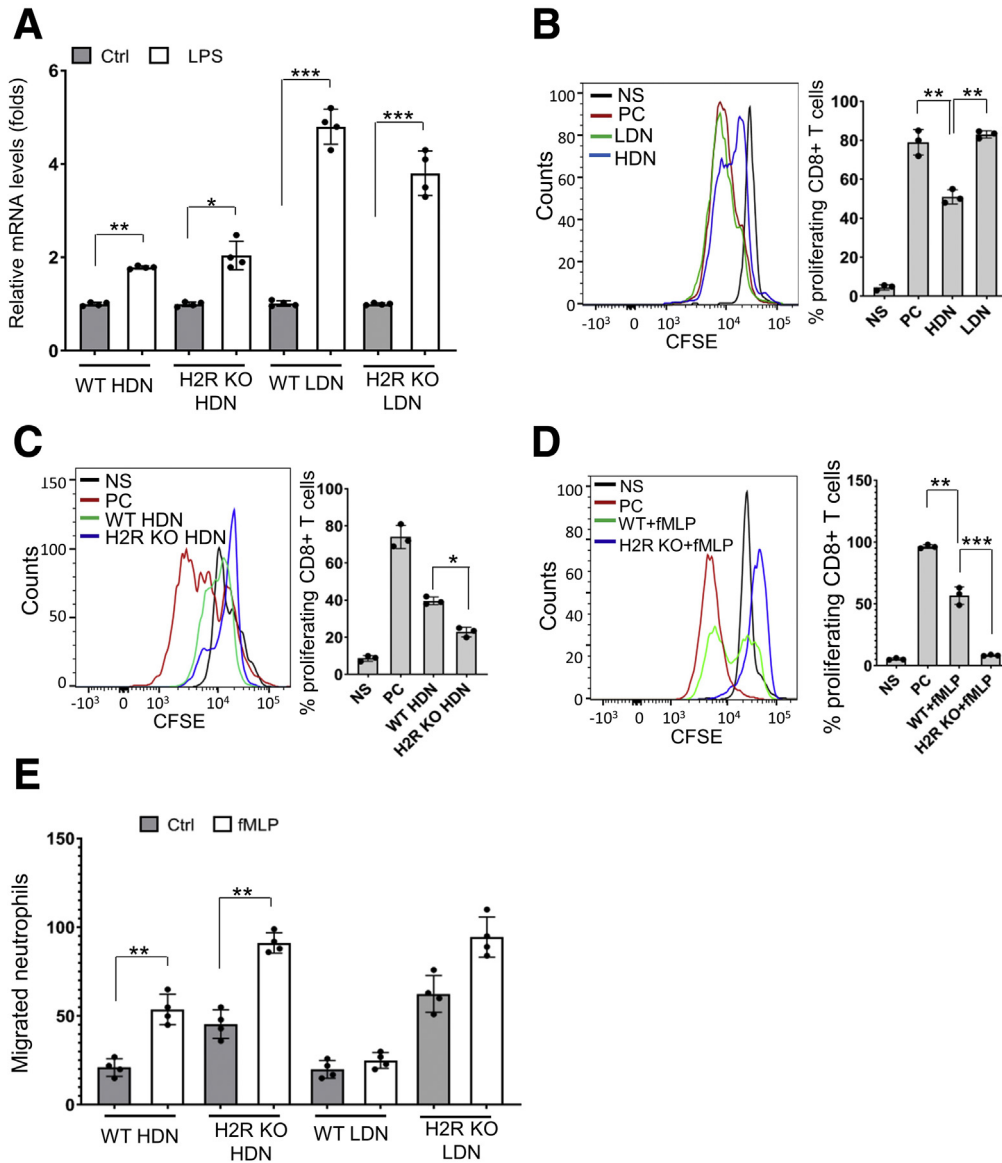
Figure 10. HDNs, not LDNs, suppressed CD8 T-cell proliferation. (A) *Cd274* messenger RNA (mRNA) levels of WT and H2R KO neutrophils treated with LPS (100 ng/mL) by qRT-PCR (n = 4). (B) Suppression of T-cell proliferation by LDNs and HDNs was determined by CFSE dilution assay using flow cytometry (n = 3). (C) Suppression of T-cell proliferation by WT and H2R KO HDNs was determined by CFSE dilution assay (n = 3). Means ± SD are shown. (D) Suppression of CD8+ T-cell proliferation by WT and H2R KO HDNs activated with fMLP (n = 3). (E) Spontaneous migration and chemotaxis of HDNs and LDNs from WT or H2R-deficient mice (n = 4). In all panels, means ± SD are shown. *P < .05, **P < .01, and ***P < .001. CFSE, Carboxyfluorescein succinimidyl ester; Ctrl, control; fMLP, N-formylmethionyl-leucyl-phenylalanine; NS, no stimulation; PC, positive control.

in tumor cells and the secretion of growth factors from neutrophils. Our findings indicated that targeted strategies to suppress H2R signaling may be a potent therapeutic strategy for cancer.

Neutrophils are major contributors to both acute and chronic inflammation and commonly are present in patients with inflammatory bowel disease, especially UC.[31] The colonic mucosa of UC patients who were hospitalized, received systemic corticosteroids, or underwent colectomy, were found to harbor an increased number of neutrophils. Neutrophil resolution has been associated with improvement of inflammation and long-term favorable outcomes for UC patients,[32] suggesting that manipulation of neutrophil function via H2R is a potentially useful treatment strategy for UC. Consistent with our data, another study has shown that oral administration of cimetidine for 1–7 days increased neutrophil counts in the peripheral blood of healthy adults.[33] In addition to yielding increased

neutrophil counts, cimetidine treatment counteracts the suppressive effect of H2R on the proinflammatory features of mature neutrophils. Our results are consistent with the studies showing that administration of H2R antagonists increased the frequency of hospitalization and surgery in patients with UC.[34,35]

The administration of cimetidine has been shown to be associated with an increased risk for multiple cancers, such as intestinal, lymphatic, and hematopoietic cancers, by several studies.[36–38] In the tumor environment, in the absence of H2R activation, mature neutrophils produce more cytokines, chemokines, ROS, and enzymes, further strengthening MDSC activity and their impact on T-cell functions. We observed a link between H2R deficiency and neutrophil IL1β levels. IL1β may promote production of PD-L1 by cancer cells.[39] Most PD-L1–expressing tumor cells were found in close proximity to H2R-deficient neutrophils in vivo, indicating that blocking H2R in neutrophils may
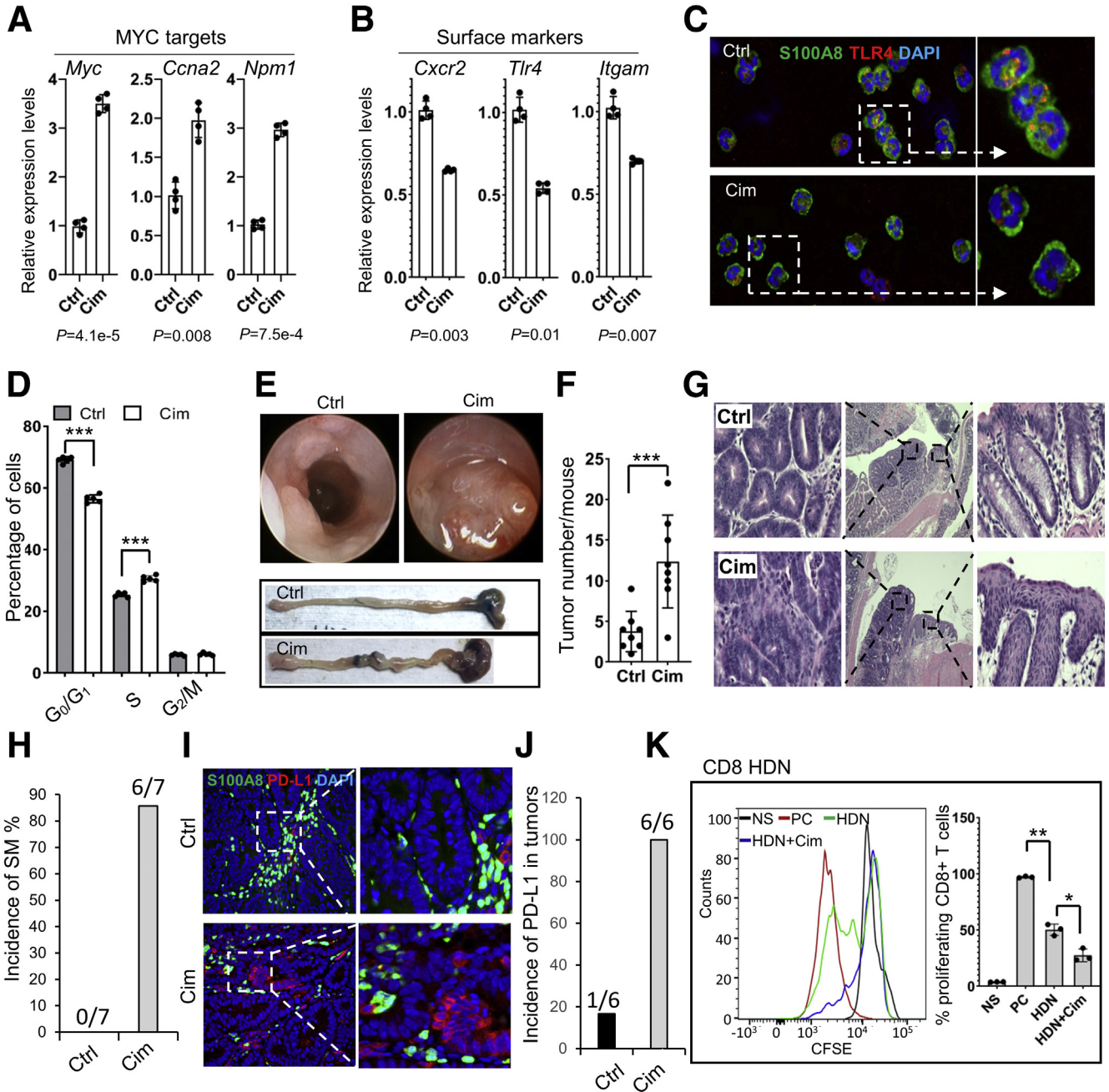
Figure 11. Cimetidine administration suppressed neutrophil maturation and promoted inflammation-associated colon cancer. (*A* and *B*) Gene expression of MYC targets and surface markers in the cimetidine-treated and control LDNs (n = 4). (*C*) Representative immunofluorescence staining (magnification: 400× and 1000×) of S100A8 (green) and TLR4 (red) in LDNs from the cimetidine-treated and control mice. (*D*) Cell-cycle analysis of bone marrow cells from the cimetidine-treated and control mice (n = 5). (*E*) Tumors in the middle colon examined by a colonoscopy (*top*), macroscopic observation of the colon (*bottom*, n = 8). (*F*) Tumor numbers counted under a dissecting microscope (n = 8). (*G* and *H*) Rectal SM was observed (magnification: 40× and 200×) after 2 cycles of DSS treatment in the cimetidine-treated mice (n = 7), but not in the control mice (n = 9). (*I* and *J*) Immunofluorescence staining (magnification: 200× and 400×) of S100A8 (green) and PD-L1 (red) in the tumors of the cimetidine-treated (n = 6) and control (n = 6) mice. (*K*) Suppression of CD8+ T-cell proliferation by cimetidine-treated and control HDNs (n = 3). All values are means ± SD. (*A* and *B*) *P* values are shown under the panels. *$P < .05$, **$P < .01$, and ***$P < .001$. Cim, cimetidine; Ctrl, control; DAPI, 4′,6-diamidino-2-phenylindole; PC, positive control.

enhance PD-L1 expression in tumor cells, promoting cancer progression. Some clinical studies have shown that after surgical removal of the primary tumor, CRC patients appeared to have an increased tumor-free survival when treated with combination therapy with cimetidine.[40] However, the results were inconsistent, making it difficult to conclude that cimetidine has any protective effect against CRC.
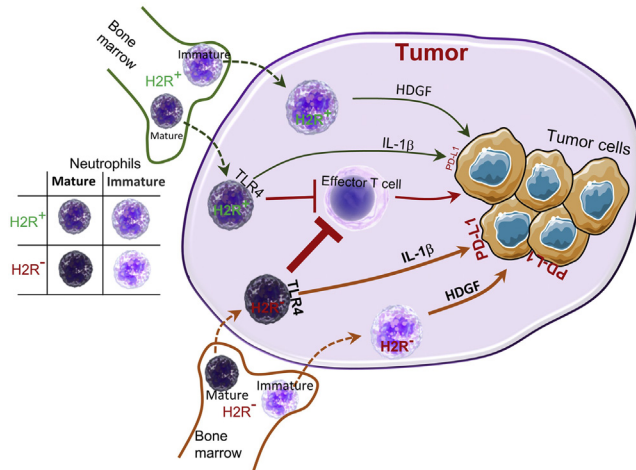
Figure 12. A model for the effects of H2R signaling on neutrophil function during tumor development. Bone marrow–derived mature and immature neutrophils infiltrate tumor tissues, contributing to cancer development by suppressing effector T cells, secreting factors including HDGF and up-regulating PD-L1 expression in tumor cells through IL1β. Disruption of H2R signaling in neutrophils enhances permissiveness toward cancer development, leading to accelerated tumor development and progression. The *thick orange arrows* indicate enhanced production, while the *thin dark green arrows* indicate baseline production.

SM is said to be related to chronic inflammation such as Crohn's disease[41] or UC.[42] Our data suggest that deactivation of H2R in neutrophils could be a key element of SM development. In mice, knockout of *Smad3* or *Smad4* can cause SM in the rectum or in the mammary glands, respectively.[43,44] Although H2R-deficient and Smad3-deficient mice showed similar phenotypes after DSS treatment, any link between H2R and Smad3 signaling still is unknown.

Histamine signaling pathways appear to be conserved between human beings and mice, with similar H2R gene expression patterns in various cell types and similar signaling cascades. We also understand the limitations of using $Apc^{min/+}$ mice to study inflammation-associated CRC, which is distinct in terms of molecular mechanisms from sporadic human CRC. CRC is known to contain a much lower frequency of *APC* mutations.[45] In this study, we focused on innate immune cells, particularly neutrophils, to gain a greater understanding of cancer cell:innate immune cell interactions in the context of colonic neoplasia. To delineate the role of H2R, which is highly expressed in neutrophils, we used a widely accepted mouse model of chronic inflammation-associated CRC by treating $Apc^{min/+}$ mice with repeated cycles of low-dose DSS. Inflammation-driven genetic alterations and epigenetic changes are involved in tumor initiation and development in both CRC and in colitis-associated colon cancer (CAC).[46] In our study, inactivation of the H2R gene alone accelerated infiltration of neutrophils and caused severe colonic inflammation as well as dysplasia after 2-cycle, low-dose DSS treatment. It also has been shown that innate immune cells can promote mutations by

producing ROS in colonic epithelial stem cells,[47,48] possibly leading to CRC initiation. Based on these findings, we believe that neutrophil-mediated mucosal inflammation may be an initiating driver in colonic neoplasia. However, human cohort studies regarding H2R signaling and targeted interventions for CRC are needed in future studies.

In conclusion, disruption of H2R signaling enhanced the tumorigenic microenvironment by supporting the relative proliferation of immature, proinflammatory, and actively proliferating neutrophils. These studies support the potential importance of innate immunity in the initiation and development of colonic neoplasia. Therefore, H2R signaling and corresponding antagonism of these pathways should be carefully considered in the context of prevention and treatment strategies for inflammatory bowel disease and CRC.

Materials and Methods
Mouse Models

Hrh2 KO mice were generated as previously described by the Genetically Modified Mouse Core at Baylor College of Medicine using clustered regularly interspaced short palindromic repeats (CRISPR)-CRISPR-associated protein 9 (Cas9) method.[49] *Hrh2* KO; $Apc^{min/+}$ double-mutant mice were generated by crossbreeding $Apc^{min/+}$ mice (C57BL/6J background) and *Hrh2* KO mice (C57BL/6J background). All mice were maintained under specific pathogen-free conditions with a 12-hour light and 12-hour dark cycle in the Feigin Tower vivarium at Texas Children's Hospital. To induce colonic inflammation, 2-month-old female mice were given 2% DSS (molecular weight, 36,000–50,000 da; MP Biomedicals, Solon, OH) in drinking water for 5 days followed by a 14-day recovery period, and a second cycle of DSS for 4 days followed by a 14-day recovery period. To test the effects of an H2R antagonist on tumor development, $Apc^{min/+}$ mice were given cimetidine (H2R antagonist, 200 mg/L) in drinking water from the start of the first cycle of DSS treatment until the end of the second recovery period. After the second recovery period, a mouse colonoscopy was performed and imaged. Mice then were killed, and the tumors in the colon were counted under a dissecting microscope. The intestinal tissues were fixed in formalin and embedded in paraffin for histologic analysis. Inflammation scores were calculated using a scoring system by combining tissue damage and inflammatory cell infiltration.[50] All procedures were approved by the Institutional Animal Care and Use Committee at Baylor College of Medicine.

Mouse Neutrophil Isolation and Purification

Mouse neutrophils were elicited, and high- and low-density neutrophils were collected according to a published protocol.[51] Briefly, 1.0 mL sterile casein solution (9%) was injected twice into the peritoneal cavity of each mouse with a 12-hour interval. Three hours after the second injection, mice were killed and neutrophils in the peritoneal cavity were recovered with 10 mL phosphate-buffered saline (PBS). The peritoneal cells were layered on a discontinuous Histopaque gradient (1.077 g/mL and 1.119 g/mL; Sigma, St. Louis, MO). High-density neutrophils were harvested from the

1.077–1.119 interface. Low-density cells, which are a heterogeneous population including neutrophils, macrophages, and lymphocytes, were harvested from the PBS-1.077 interface. The low-density neutrophils were purified further using a MojoSort Mouse Neutrophil Isolation Kit (BioLegend, San Diego, CA). The neutrophil purity was confirmed by flow cytometry using anti-CD11b, Ly6G antibodies (Table 1). Neutrophils were identified as $CD11b^+$ $Ly6G^+$ cells.

T-Cell Suppression

Mouse $CD3^+$ T cells were purified from splenocytes of WT mice using a negative selection kit (BioLegend). Cells were stained with 10 umol/L Carboxyfluorescein succinimidyl ester (CFSE, Sigma) in PBS containing 0.1% bovine serum albumin at 37°C for 10 minutes, washed with cold RPMI-1640, and resuspended with X-VIVO 15 Serum-free Hematopoietic Cell Medium (Walkersville, MD). Cells then were seeded onto 96-well plates coated with CD3 (5 μg/mL) and CD28 (5 μg/mL) at 5×10^4/well. The same number of neutrophils was added to each well. Cells were treated with N-acetylcysteine (1 mmol/L; Sigma), fMLP (1 μmol/L; Sigma), or left untreated as a control. After 5 days of incubation at 37°C, the proliferative capacity of T cells ($CD4^+$ and $CD8^+$) was analyzed by flow cytometry based on CFSE signal in a fluorescein isothiocyanate channel.

Neutrophil Chemotaxis

Neutrophil chemotaxis was determined using a disposable chemotaxis system (Neuro Probe, Bethesda, MD) with a 3-μm pore filter membrane. fMLP (1 μmol/L) in Dulbecco's modified Eagle medium or media control was added to the lower chamber compartment. Mouse neutrophils (1×10^5 cells in 30 μL) were seeded on the top of the 3-μm pore filter membrane. The plate was incubated for 1 hour at 37°C in a 5% CO_2 incubator. The neutrophils that had migrated into the lower chamber were counted using an automated cell counter (Invitrogen, Grand Island, NY).

Cell-Cycle Analysis

Bone marrow cells from 2-month-old female mice were obtained by flushing the femurs with sterile PBS, and then the bone marrow cells were passed through 70-μm filters. Cells were fixed with 70% cold ethanol at 4°C overnight. After being washed with cold PBS twice, the cells were treated with 0.2 μg/mL RNase A (Qiagen, Valencia, CA), and then stained with 0.5 μg/mL propidium iodide (Sigma) in the dark for 30 minutes at room temperature. DNA content was determined by a FACSCanto flow cytometer (BD Biosciences, San Jose, CA) and percentages of cells in different phases of the cell cycle were assessed. The distribution of cells at different cell-cycle phases was analyzed using the model included in the ModFit LTTM (Verity Software House, Topsham, ME) software program.

MagPix Analysis of Cytokines

Supernatants from neutrophils were assayed using a cytokine magnetic bead panel (cat. MCYTOMAG-70K; Millipore, Billerica, MA) with a MagPix instrument according to the manufacturer's protocol. Raw data were obtained with a Luminex Corporation (Austin, TX) xPONENT for MagPix (version 4.2) and analyzed with MILLIPLEX Analyst (version 5.1.0.0, Billerica, MA).

Table 1. Antibody Information

Antibody	Company	Cat#	Applications and dilutions
S100A8	Novus Biologicals, Littleton, CO	MAB3059	Fluorescent staining 1:300
PCNA	Santa Cruz, Dallas, TX	sc56	Fluorescent staining 1:100
MUC2	Invitrogen	PA5-21329	Fluorescent staining 1:200
PD-L1	R&D Systems	AF1019-SP	Fluorescent staining 1:100
SMA	Sigma	SAB5500002	Fluorescent staining 1:100
CXCR2	Thermo Fisher	PA5-100951	Fluorescent staining 1:100
TLR4	Novus Biologicals	NB100-56566SS	Fluorescent staining 1:100
IL1b	Abcam, Cambridge, MA	Ab9722	Fluorescent staining 1:100
p-iκBα	Cell Signaling, Danvers, MA	9246	Western blot 1:1000
p-ERK	Cell Signaling	9101	Western blot 1:1000
ERK	Cell Signaling	9102	Western blot 1:1000
p-p38	Cell Signaling	9215	Western blot 1:1000
p38	Cell Signaling	9212	Western blot 1:1000
PKA substrate	Cell Signaling	9621	Western blot 1:1000
β-actin	Sigma	A1978	Western blot 1:5000
CD8	BioLegend	300912	Flow cytometry 1:200
CD4	BioLegend	317427	Flow cytometry 1:200
Ly6G	BD Biosciences	551460	Flow cytometry 1:200
CD11b	Thermo Fisher	12-0112-82	Flow cytometry 1:200

CXCR2, C-X-C Motif Chemokine Receptor 2; MUC2, Mucin 2; p-ERK, **phosphorylated** ERK; p-iκBα, **phosphorylated iκBα**; PCNA, proliferating cell nuclear antigen; PKA, adenosine 3′,5′-cyclic monophosphate–dependent protein kinase; SMA, Smooth muscle actin.

Immunofluorescence Staining

Immunofluorescence was performed on 5-μm–thick, formalin-fixed, paraffin-embedded slides that were deparaffinized with xylene, hydrated with a series of washes using graded alcohols, followed by heat-induced antigen retrieval with Tris-EDTA buffer (pH 8.0, 1 mmol/L EDTA, 10 mmol/L Tris) for 30 minutes. After a PBS wash, slides were blocked with 10% goat sera for 30 minutes, and then incubated with primary antibodies (Table 1) in Tris Buffered Saline with Tween 20 (TBS-T) buffer at 4°C overnight. After washing with TBS-T, slides were incubated with Alexa Fluor–conjugated secondary antibodies (Invitrogen, Carlsbad, CA) (Table 1) for 60 minutes, followed by 4',6-diamidino-2-phenylindole counterstaining and imaging by fluorescence microscopy (Nikon, Tokyo, Japan). Antibodies are listed in Table 1.

Immunoblots

Neutrophils were lysed with RIPA buffer (Thermo Fisher Scientific, Waltham, MA) containing a protease inhibitor cocktail (Roche, Indianapolis, IN). After centrifugation, the supernatants were resolved by sodium dodecyl sulfate–polyacrylamide gel electrophoresis and transferred to polyvinylidene difluoride membranes (Millipore). The membranes were blocked with 5% dry milk in TBS-T for 30 minutes, washed with TBS-T, and then incubated with primary antibodies overnight at 4°C. After 3 washes with TBS-T, the membranes were incubated with horseradish peroxidase–conjugated secondary antibodies for 1 hour at room temperature, and developed with Enhanced chemiluminescence (ECL) substrate (GE Health Care, Buckinghamshire, UK) after TBS-T washes.

RNA Extraction, RNA Sequencing, and qRT-PCR Analysis

Total RNA was extracted using TRIzol reagent (Life Technologies, Gaithersburg, MD) followed by purification with a RNeasy Mini Kit (Qiagen). RNA sequencing was performed at Genewiz (South Plainfield, NJ). The RNA samples that met the criteria for sequencing were processed for library preparation using standard Illumina protocols. High-throughput paired-end (2 × 150 bp) sequencing was performed on a HiSeq platform (Illumina, San Diego, CA). Sequencing reads were trimmed to remove possible adapter sequences and nucleotides with poor quality using Trimmomatic v.0.36. The trimmed reads were mapped to the *Mus musculus* GRCm38 reference genome available on ENSEMBL using the STAR aligner v.2.5.2b. The STAR aligner is a splice aligner that detects splice junctions and incorporates them to help align the entire read sequences. Binary Alignment Mapping (BAM) files were generated as a result. Complementary DNA was prepared with 1 μg total RNA using the SensiFAST Complementary DNA Synthesis kit (Bioline, Taunton, MA). Quantitative PCR then was performed using Fast SYBR Green (Life Technologies) on an Applied Biosystems 7900HT instrument (Foster City, CA). Ribosomal RNA (18S) was used as a control. Primers are included in Table 2. Relative levels of gene expression were

Table 2.	Primer Information		
Gene name	**Sequence**	**Gene name**	**Sequence**
Hrh1 F	ATCCTGTTTGCTCAGCCACT	*Itgam* F	ATGGACGCTGATGGCAATACC
Hrh1 R	CCTGGATCTCCACAGCAGTT	*Itgam* R	TCCCCATTCACGTCTCCCA
Hrh2 F	CAGAAAGAGTAGCCAGTAGTG	*Cebpb* F	TCTACTACGAGCCCGACTG
Hrh2 R	TGTATCTTGAGGTGGCTTAGG	*Cebpb* R	GGGCTGAAGTCGATGGC
Myc F	CCCTATTTCATCTGCGACGAG	*Cebpd* F	CGACTTCAGCGCCTACATTGA
Myc R	GAGAAGGACGTAGCGACCG	*Cebpd* R	CTAGCGACAGACCCCACAC
Ccna2 F	GCCTTCACCATTCATGTGGAT	*Cebpe* F	CTGGGGAAGAACAGCTACTTTC
Ccna2 R	TTGCTGCGGGTAAAGAGACAG	*Cebpe* R	GTGAGGGATAGGCGAATGGC
Npm1 F	ATGGAAGACTCGATGGATATGGA	*Cd274* F	AGTATGGCAGCAACGTCACG
Npm1 R	ACCGTTCTTAATGACAACTGGTG	*Cd274* R	TCCTTTTCCCAGTACACCACTA
Rela F	AGGCTTCTGGGCCTTATGTG	*S100a8* F	AAATCACCATGCCCTCTACAAG
Rela R	TGCTTCTCTCGCCAGGAATAC	*S100a8* R	CCCACTTTTATCACCATCGCAA
Relb F	CCGTACCTGGTCATCACAGAG	*S100a9* F	GCACAGTTGGCAACCTTTATG
Relb R	CAGTCTCGAAGCTCGATGGC	*S100a9* R	TGATTGTCCTGGTTTGTGTCC
Il1b F	GCAACTGTTCCTGAACTCAACT	*Hdgf* F	CCGGATTGATGAGATGCCTGA
Il1b R	ATCTTTTGGGGTCCGTCAACT	*Hdgf* R	TTGCCAAACTTCTCCTTGGATT
Cxcr2 F	GCCCTGCCCATCTTAATTCTAC	*Il1r1* F	TGGTACAAGAATGACAGCAAGA
Cxcr2 R	ATACGCAGTACGACCCTCAA	*Il1r1* R	TGGCAGGTACAAACCAAAGA
Tlr4 F	GGACTCTGATCATGGCACTG		
Tlr4 R	TGTCATCAGGGACTTTGCTG		

F, forward; R, reverse.

analyzed using the comparative threshold cycle (CT) method (2-ΔΔCT method).

Flow Cytometry

Neutrophils were incubated first with Fc-block (BD Biosciences) in 100 μL PBS at 4°C for 15 minutes and then with antibodies (Table 1) at 4°C for 30 minutes in the dark. The cells were washed in PBS, spun down, and resuspended with 200 μL PBS. The cell samples were examined using a FACSCanto flow cytometer (BD Biosciences), and data were analyzed using FlowJo software (version10.5.3; FlowJo LLC, Ashland, OR).

Colonoid Culture

The procedure of colonoid culture was modified from the protocol described by Fernando et al.[52] Briefly, mouse colon was cut into approximately 1-cm pieces and washed with cold PBS for 5 minutes at 4°C with end-to-end shaking. The tissues then were incubated in cold PBS containing 3 mmol/L EDTA, dithiothreitol, and sucrose for 30 minutes at 4°C with shaking. After vigorous shaking with cold PBS, the crypts were pelleted and embedded in Matrigel (Corning, Tewksbury, MA). After incubation for 20 minutes at 37°C, the solidified Matrigel was overlaid with complete crypt culture media containing Epidermal growth factor (EGF) (50 ng/mL; R&D Systems, Minneapolis, MN) and 10 μmol/L Y-27632 (Sigma), an inhibitor of Rho-associated protein kinase, to block apoptosis.

Statistical Analysis

Statistical analysis was performed using GraphPad Prism version 5.04, and statistical significance was determined by an unpaired, 2-tailed, Student t test or 1-way analysis of variance as follows: $*P < .05$, $**P < .01$, and $***P < .001$.

References

1. Branco A, Yoshikawa FSY, Pietrobon AJ, Sato MN. Role of histamine in modulating the immune response and inflammation. Mediat Inflamm 2018;2018:9524075.

2. Gao C, Major A, Rendon D, Major A, Rendon D, Lugo M, Jackson V, Shi Z, Mori-Akiyama Y, Versalovic J. Histamine H2 receptor-mediated suppression of intestinal inflammation by probiotic Lactobacillus reuteri. mBio 2015;6:e01358-15.

3. Shi Z, Fultz RS, Engevik MA, Gao C, Hall A, Major A, Mori-Akiyama Y, Versalovic J. Distinct roles of histamine H1- and H2-receptor signaling pathways in inflammation-associated colonic tumorigenesis. Am J Physiol Gastrointest Liver Physiol 2019;316:G205–G216.

4. Yang XD, Ai W, Asfaha S, Bhagat G, Friedman RA, Jin G, Park H, Shykind B, Diacovo TG, Falus A, Wang TC. Histamine deficiency promotes inflammation-associated carcinogenesis through reduced myeloid maturation and accumulation of CD11b+Ly6G+ immature myeloid cells. Nat Med 2011;17:87–95.

5. Youn JI, Nagaraj S, Collazo M, Nagaraj S, Gabrilovich DI. Subsets of myeloid-derived suppressor cells in tumor-bearing mice. J Immunol 2008;181:5791–5802.

6. Aarts CEM, Kuijpers TW. Neutrophils as myeloid-derived suppressor cells. Eur J Clin Invest 2018;48(Suppl 2): e12989.

7. Srivastava MK, Sinha P, Clements VK, Rodriguez P, Ostrand-Rosenberg S. Myeloid-derived suppressor cells inhibit T-cell activation by depleting cystine and cysteine. Cancer Res 2010;70:68–77.

8. Bowers NL, Helton ES, Huijbregts RP, Goepfert PA, Heath SL, Hel Z. Immune suppression by neutrophils in HIV-1 infection: role of PD-L1/PD-1 pathway. PLoS Pathog 2014;10:e1003993.

9. Tao J, Han D, Gao S, Zhang W, Yu H, Liu P, Fu R, Li L, Shao Z. CD8(+) T cells exhaustion induced by myeloid-derived suppressor cells in myelodysplastic syndromes patients might be through TIM3/Gal-9 pathway. J Cell Mol Med 2020;24:1046–1058.

10. Li Z, Wang J, Zhang X, Liu P, Zhang X, Wang J, Zheng X, Wei L, Peng Q, Liu C, Yan Q, Shen S, Li X, Ma J. Proinflammatory S100A8 induces PD-L1 expression in macrophages, mediating tumor immune escape. J Immunol 2020;204:2589–2599.

11. Vogl T, Tenbrock K, Ludwig S, Leukert N, Ehrhardt C, van Zoelen MA, Nacken W, Foell D, van der Poll T, Sorg C, Roth J. Mrp8 and Mrp14 are endogenous activators of Toll-like receptor 4, promoting lethal, endotoxin-induced shock. Nat Med 2007;13:1042–1049.

12. Huang M, Wu R, Chen L, Peng Q, Li S, Zhang Y, Zhou L, Duan L. S100A9 regulates MDSCs-mediated immune suppression via the RAGE and TLR4 signaling pathways in colorectal carcinoma. Front Immunol 2019;10:2243.

13. Grauers Wiktorin H, Nilsson MS, Kiffin R, Sander FE, Lenox B, Rydstrom A, Hellstrand K, Martner A. Histamine targets myeloid-derived suppressor cells and improves the anti-tumor efficacy of PD-1/PD-L1 checkpoint blockade. Cancer Immunol Immunother 2019; 68:163–174.

14. Patrone F, Dallegri F, Lanzi G, Sacchetti C. Reversal by cimetidine of histamine-induced inhibition of true chemotaxis in neutrophil polymorphonuclears. Res Exp Med (Berl) 1980;176:201–205.

15. Flamand N, Plante H, Picard S, Laviolette M, Borgeat P. Histamine-induced inhibition of leukotriene biosynthesis in human neutrophils: involvement of the H2 receptor and cAMP. Br J Pharmacol 2004;141:552–561.

16. Betten A, Dahlgren C, Hermodsson S, Hellstrand K. Histamine inhibits neutrophil NADPH oxidase activity triggered by the lipoxin A4 receptor-specific peptide agonist Trp-Lys-Tyr-Met-Val-Met. Scand J Immunol 2003;58:321–326.

17. Zisman TL, Rubin DT. Colorectal cancer and dysplasia in inflammatory bowel disease. World J Gastroenterol 2008;14:2662–2669.

18. Ullman TA, Itzkowitz SH. Intestinal inflammation and cancer. Gastroenterology 2011;140:1807–1816.

19. Ramai D, Changela K, Lai J, Shahzad G, Reddy M. Interval squamous cell carcinoma of the rectum. Case Rep Gastroenterol 2017;11:396–401.

20. Cooper HS, Everley L, Chang WC, Pfeiffer G, Lee B, Murthy S, Clapper ML. The role of mutant Apc in the

development of dysplasia and cancer in the mouse model of dextran sulfate sodium-induced colitis. Gastroenterology 2001;121:1407–1416.

21. Nalbantoglu I, Blanc V, Davidson NO. Characterization of colorectal cancer development in Apc (min/+) mice. Methods Mol Biol 2016;1422:309–327.

22. Valentini AM, Di Pinto F, Cariola F, Guerra V, Giannelli G, Caruso ML, Pirrelli M. PD-L1 expression in colorectal cancer defines three subsets of tumor immune microenvironments. Oncotarget 2018;9:8584–8596.

23. Silvestre-Roig C, Fridlender ZG, Glogauer M, Scapini P. Neutrophil diversity in health and disease. Trends Immunol 2019;40:565–583.

24. Coffelt SB, Wellenstein MD, de Visser KE. Neutrophils in cancer: neutral no more. Nat Rev Cancer 2016; 16:431–446.

25. Schmielau J, Finn OJ. Activated granulocytes and granulocyte-derived hydrogen peroxide are the underlying mechanism of suppression of T-cell function in advanced cancer patients. Cancer Res 2001; 61:4756–4760.

26. Kishimoto Y, Asakawa S, Sato T, Takano T, Nakajyo T, Mizuno N, Segawa R, Yoshikawa T, Hiratsuka M, Yanai K, Ohtsu H, Hirasawa N. Induced histamine regulates Ni elution from an implanted Ni wire in mice by downregulating neutrophil migration. Exp Dermatol 2017;26:868–874.

27. Lawrence SM, Corriden R, Nizet V. The ontogeny of a neutrophil: mechanisms of granulopoiesis and homeostasis. Microbiol Mol Biol Rev 2018;82:e00057-17.

28. Chen X, Deng H, Churchill MJ, Luchsinger LL, Du X, Chu TH, Friedman RA, Middelhoff M, Ding H, Tailor YH, Wang ALE, Liu H, Niu Z, Wang H, Jiang Z, Renders S, Ho SH, Shah SV, Tishchenko P, Chang W, Swayne TC, Munteanu L, Califano A, Takahashi R, Nagar KK, Renz BW, Worthley DL, Westphalen CB, Hayakawa Y, Asfaha S, Borot F, Lin CS, Snoeck HW, Mukherjee S, Wang TC. Bone marrow myeloid cells regulate myeloid-biased hematopoietic stem cells via a histamine-dependent feedback loop. Cell Stem Cell 2017; 21:747–760 e7.

29. Satoh Y, Matsumura I, Tanaka H, Ezoe S, Sugahara H, Mizuki M, Shibayama H, Ishiko E, Ishiko J, Nakajima K, Kanakura Y. Roles for c-Myc in self-renewal of hematopoietic stem cells. J Biol Chem 2004;279:24986–24993.

30. Lian J, Tang J, Shi H, Li H, Zhen T, Xie W, Zhang F, Yang Y, Han A. Positive feedback loop of hepatoma-derived growth factor and beta-catenin promotes carcinogenesis of colorectal cancer. Oncotarget 2015; 6:29357–29374.

31. Muthas D, Reznichenko A, Balendran CA, Bottcher G, Clausen IG, Karrman Mardh C, Ottosson T, Uddin M, MacDonald TT, Danese S, Berner Hansen M. Neutrophils in ulcerative colitis: a review of selected biomarkers and their potential therapeutic implications. Scand J Gastroenterol 2017;52:125–135.

32. Pai RK, Hartman DJ, Rivers CR, Regueiro M, Schwartz M, Binion DG, Pai RK. Complete resolution of

mucosal neutrophils associates with improved long-term clinical outcomes of patients with ulcerative colitis. Clin Gastroenterol Hepatol 2020;18:2510–2517.e5.

33. Asakage M, Tsuno NH, Kitayama J, Yamada J, Tsuchiya T, Yoneyama S, Takahashi K, Nagawa H. [The effect of cimetidine mainly increases CD4+ cells of peripheral blood T lymphocytes]. Gan To Kagaku Ryoho 2005;32:1576–1577.

34. Juillerat P, Schneeweiss S, Cook EF, Ananthakrishnan AN, Mogun H, Korzenik JR. Drugs that inhibit gastric acid secretion may alter the course of inflammatory bowel disease. Aliment Pharmacol Ther 2012;36:239–247.

35. Shah R, Richardson P, Yu H, Kramer J, Hou JK. Gastric acid suppression is associated with an increased risk of adverse outcomes in inflammatory bowel disease. Digestion 2017;95:188–193.

36. Moller H, Lindvig K, Klefter R, Mosbech J, Moller Jensen O. Cancer occurrence in a cohort of patients treated with cimetidine. Gut 1989;30:1558–1562.

37. Colin-Jones DG, Langman MJ, Lawson DH, Vessey MP. Postmarketing surveillance of the safety of cimetidine: 12 month mortality report. Br Med J (Clin Res Ed) 1983; 286:1713–1716.

38. Habel LA, Levin TR, Friedman GD. Cimetidine use and risk of breast, prostate, and other cancers. Pharmacoepidemiol Drug Saf 2000;9:149–155.

39. Zheng SLQ, Ma R. IL-1β up-regulates PD-L1 via STAT3-dependent and independent mechanism in esophageal squamous cell carcinoma. Eur J Immunol 2019;49: 3054.

40. Deva S, Jameson M. Histamine type 2 receptor antagonists as adjuvant treatment for resected colorectal cancer. Cochrane Database Syst Rev 2012;8:CD007814.

41. Langner C, Wenzl HH, Bodo K, Petritsch W. Squamous metaplasia of the colon in Crohn's disease. Histopathology 2007;51:556–557.

42. Maruoka T, Hasegawa K, Nagasako K. Squamous cell metaplasia without dysplasia of the colonic mucosa in ulcerative colitis. Gastrointest Endosc 1990;36: 65–66.

43. Seamons A, Treuting PM, Brabb T, Maggio-Price L. Characterization of dextran sodium sulfate-induced inflammation and colonic tumorigenesis in Smad3(-/-) mice with dysregulated TGFbeta. PLoS One 2013;8: e79182.

44. Li W, Qiao W, Chen L, Xu X, Yang X, Li D, Li C, Brodie SG, Meguid MM, Hennighausen L, Deng CX. Squamous cell carcinoma and mammary abscess formation through squamous metaplasia in Smad4/Dpc4 conditional knockout mice. Development 2003; 130:6143–6153.

45. Baker AM, Cross W, Curtius K, Al Bakir I, Choi CR, Davis HL, Temko D, Biswas S, Martinez P, Williams MJ, Lindsay JO, Feakins R, Vega R, Hayes SJ, Tomlinson IPM, McDonald SAC, Moorghen M, Silver A, East JE, Wright NA, Wang LM, Rodriguez-Justo M, Jansen M, Hart AL, Leedham SJ, Graham TA.

Evolutionary history of human colitis-associated colorectal cancer. Gut 2019;68:985–995.

46. Terzic J, Grivennikov S, Karin E, Karin M. Inflammation and colon cancer. Gastroenterology 2010; 138:2101–2114 e5.

47. Meira LB, Bugni JM, Green SL, Lee CW, Pang B, Borenshtein D, Rickman BH, Rogers AB, Moroski-Erkul CA, McFaline JL, Schauer DB, Dedon PC, Fox JG, Samson LD. DNA damage induced by chronic inflammation contributes to colon carcinogenesis in mice. J Clin Invest 2008;118:2516–2525.

48. Westbrook AM, Wei B, Braun J, Schiestl RH. Intestinal mucosal inflammation leads to systemic genotoxicity in mice. Cancer Res 2009;69:4827–4834.

49. Fultz R, Engevik MA, Shi Z, Hall A, Herrmann B, Ganesh BP, Major A, Haag A, Mori-Akiyama Y, Versalovic J. Phagocytosis by macrophages depends on histamine H2 receptor signaling and scavenger receptor 1. Microbiologyopen 2019;8:e908.

50. Wirtz S, Popp V, Kindermann M, Gerlach K, Weigmann B, Fichtner-Feigl S, Neurath MF. Chemically induced mouse models of acute and chronic intestinal inflammation. Nat Protoc 2017;12:1295–1309.

51. Swamydas M, Luo Y, Dorf ME, Lionakis MS. Isolation of mouse neutrophils. Curr Protoc Immunol 2015;110:3–20, 1–3.20.15.

52. Fernando EH, Dicay M, Stahl M, Gordon MH, Vegso A, Baggio C, Alston L, Lopes F, Baker K, Hirota S, McKay DM, Vallance B, MacNaughton WK. A simple, cost-effective method for generating murine colonic 3D enteroids and 2D monolayers for studies of primary epithelial cell function. Am J Physiol Gastrointest Liver Physiol 2017;313:G467–G475.

Correspondence
Address correspondence to: James Versalovic, MD, PhD, Department of Pathology, Texas Children's Hospital, 1102 Bates Avenue, Suite 830, Houston, Texas 77030. e-mail: jamesv@bcm.edu; fax: (832) 825-1165.